

Professor Nga Lee (Sally) Ng  
Co-Editor of Atmospheric Chemistry and Physics

5 Dear Sally,

Listed below are our responses to the comments from the reviewers of our manuscript. We thank the reviewers for carefully reading our manuscript and for their very helpful suggestions! For clarity and visual distinction, the referee comments or questions are listed here in black and are preceded by bracketed, italicized numbers (e.g. *[1]*). Authors' responses are in red below each referee statement with matching numbers (e.g. *[A1]*).

Sincerely,

15 Allan Bertram  
Professor of Chemistry  
University of British Columbia

20 Anonymous Referee #1

Maclean et al. has estimated mixing times of organic molecules within secondary organic aerosol particles. In chemical transport models SOA particles are often assumed to be homogeneously well-mixed on the timescale of <1h, which could be in question if SOA particles adopt glassy or amorphous semisolid states. Combining laboratory data, meteorological conditions, and chemical transport modeling, this study predicted that mixing times should be indeed within <1h in the planetary boundary layer. They concluded that the assumption of well-mixed SOA in chemical transport models seems reasonable for biogenic SOA in most locations in the PBL. This is a very interesting study, the method seems reasonable, and the manuscript is clearly written and easy to follow. I have several comments as below, which should be implemented in the revised manuscript before publication in ACP.

35 *[1]* The analysis is focused on 200nm-diameter particles and I agree that this may be most frequent size to be observed in ambient environments. Aged particles can have much larger diameters of up to 1  $\mu\text{m}$ , as observed for example in remote areas or Tokyo (see Fig. 7 in Takegawa et al., J. Geophys. Res., 111, D11206, 2006). Thus, I would suggest that the same analysis should be conducted with a larger diameter, say 500 nm-diameter particles. Then same figures of Fig. 3 could be presented and lines can be added in Fig. 4 (if the results are too similar with 200 nm, then they can be placed in the supplement/appendix). Mixing times should be larger for larger particles and I would be curious to know if mixing timescales would be still below 1 h. This should be easy and straightforward to do for authors and it will certainly strengthen their conclusion.

45

[A1] *To address the referee's comments we have calculated mixing times for 500 nm-diameter particles as suggested and added the results to the revised manuscript. See Section 3.4 and Figure S3 in the revised manuscript.*

5 [2] It is very interesting to compare Fig. 6 in this study with Fig. 3d in Shiraiwa et al. (Nat. Commun., 8:15002, 2017). Shiraiwa et al. predicted the glass transition temperatures of SOA in a global model and estimated mixing timescales using annual average of RH and T for 2005-2009, while this study considers seasonal dependence, but did not simulate Tg or viscosity directly but viscosity was parameterized based on  $\alpha$ -pinene viscosity  
10 measurements. I think there should be some discussion with a paragraph or two comparing these two studies. General trends seem to be consistent: longer timescales in west US, Sahara, and Mideast and shorter timescales in Europe and higher latitudes (Why there are no information over some places, such as Europe in panel a and over Amazon in both panels?). However, this study seems to estimate mixing timescales  
15 shorter in general. Please add some discussions.

[A2] *In the revised manuscript, we have added a new section (Section 3.7) where we compared our studies with the studies by Shiraiwa et al. as suggested.*

20 [3] - Abstract, L23: "SOA concentrations are significant." is ambiguous. I suggest being specific here ( $> 0.5 \text{ ug m}^{-3}$ ).

[A3] *This change has been made as suggested.*

25 [4] - P2, L4: I suggest replacing "the lowest" to "low". Not only the lowest ones, but low and semivolatile products would also condense.

[A4] *This change has been made as suggested.*

30 [5] - P5, L3: "under predict" should be "underpredict".

[A5] *This change has been made as suggested.*

[6] - Figure 6 is not very easy to read and I feel this is because of overlapping yellow lines, arrows, and letters. Can you just remove these yellow things, and just put colors for places with SOA concentrations above  $0.5 \text{ ug m}^{-3}$ ? This would improve accessibility of this important figure.  
35

[A6] *This change has been made as suggested.*

40 [7] - It may be good and helpful for readers to have a summary/conclusion section in the end of the manuscript.

[A7] *A summary/conclusion section has been added as suggested. See Section 4.0 in the revised manuscript.*  
45

[8] - I suggest combining Section S1 with the main text, or include it as Appendix (particularly bring eq S1 and S2).

[A8] *This change has been made.*

5

[9] - I would suggest moving Fig. S3, S4 (also S5?) in the main text (maybe in Appendix?). There seem to be non-negligible cases with mixing timescales >1 h for anthropogenic SOA (given that sucrose is a good proxy for that).

10

[A9] *If possible, we would prefer to keep these figures in the Supplement to avoid making the main document too long. However, we can move these figures to the main text if the Editor prefers.*

15

Anonymous Referee #2

[10] The authors report on mixing timescales within SOA particles using a parameterization that is developed based on literature data. They conclude that within the planetary boundary layer biogenic SOA particles can usually be considered well-mixed, having mixing timescales < 1h. Their work has potentially important implications for thinking about how air quality and climate models treat SOA formation and addresses an important topic. My major concerns relate to the robustness of the parameterization and how this might impact the conclusions here, especially in the context of (i) the exceptionally different, and still unexplained, viscosities between the Grayson et al. and Zhang et al. studies, the key ones for this work and (ii) the uncertainty within an individual study of SOA viscosity. I do not find that the current work sufficiently addresses the question of robustness, even with the sensitivity test that is included. Associated, I have concerns that their statement that none of their conclusions are significantly impacted by data uncertainty is not sufficiently justified. Specific comments are below.

20  
25  
30

[A10] *Thank you for raising these important and excellent questions/comments. We have addressed these questions/comments below.*

35

[11] Fig. 1: Given that the parametrization depends on RH and T, it would be useful if Fig. 1 were augmented with additional panels showing the average PBL RH and T as a function of lat/lon.

[A11] *As suggested, we have added figures to the revised manuscript (Figures S1 and S2) that show global maps of the average RH and T for January and July at the Earth's surface and the top of the planetary boundary layer.*

40

[12] P3/L19: Looking at Fig. 2, it is difficult to fully understand the parameterization that has been developed. It seems apparent that the viscosity of the  $\alpha$ -pinene SOA measured at 293 K at a given RH differs dramatically between studies, with the reported values varying over orders of magnitude. (I'm comparing the "brown" circles to the more red

45

“stars and pentagons.”) In fact, the authors acknowledge this fact in section 3.4 (“Sensitivity analysis...”), and attempt to address it. However, I have substantial concerns, nonetheless. First, it is evident from Fig. 3 that the vast majority of the observations are in the T-range 290-300 K. This is the range of both the Grayson and Zhang observations. The Zhang et al. observations indicate that the viscosity at 293 K and 58% RH is  $1 \times 10^7$  Pa s, which translates to a mixing time of 5 h for a 200 nm diameter particle. A condition of 58% RH and  $T = 293$  K is very close to the high probability region in Fig. 2B (July). Thus, it would seem that the probability of having mixing time scales  $>1$  h in July (based on Zhang et al.) would be substantial, much more than indicated by the authors in Section 3.4. Most likely, this is because of the incorporation of the Jarvinen et al. low-T data, which appears to have a similar viscosity as the SOA from Zhang et al. at the same RH but a much lower temperature. Including the Jarvinen data, which is at temperatures well-below the most probable range, leads to the parameterized viscosity at this most probable (July) condition being underestimated relative to if only the Zhang et al. observations were used. (This is difficult to assess because the authors do not provide a Figure similar to Fig. 2 that shows the Grayson-excluded parameterization, nor do they provide their best fit parameters.) I suggest that the inclusion of histograms for the alternative (sensitivity) case, similar to Fig. 4, is necessary. Additionally, I strongly suggest that a sensitivity case that excludes the pure water observations in developing the parametrization is needed. With this, the Grayson et al. and Zhang et al. results should be considered separately. This would require ignoring any T-dependence, but as most of the RH/T pairs overlap with these data sets, and the variability in RH is much greater than the variability in T, it would be a reasonable approximation. The authors must show the contours associated with their alternative parameterizations (as they do in Fig. 2 for their reference case).

*[A12] To address the referee's concerns, in the revised manuscript, we have first focused on a parameterization that just includes the room-temperature and low-temperature viscosity data from Grayson et al. and Jarvinen et al., which corresponds to SOA generated at high mass concentrations. See Sections 3.1-3.4 in the revised manuscript. Then, we focused on a parameterization that just includes the SOA room-temperature viscosity data from Zhang et al., which corresponds to SOA generated under low mass concentrations. See Section 3.5 in the revised manuscript.*

[13] Further, while I appreciate the sensitivity test that was done, it should be noted that the reported uncertainty in the Zhang et al. measurements is  $\pm 2$  orders of magnitude. At the high end, this would imply that SOA in much of the atmosphere would not mix on a 1 h time scale. On the low end, nearly all SOA would always be well mixed. This is because a 1 h mixing time scale corresponds approximately to a viscosity of  $2 \times 10^6$  Pa s, and thus variability around this value can have a large impact on the conclusions; the uncertainties on the Zhang et al. measurements overlap this critical value up to an RH of 58%.

*[A13] In the revised manuscript, uncertainties in the viscosity data have been considered in the sensitivity analysis. See Section 3.4 and Figure S4 in the revised manuscript. The*

*sensitivity analysis was performed using the upper viscosity limits of the Grayson et al. data and the upper RH limits of the Järvinen et al. data.*

[14] Continuing with this, the results from Grayson et al. also suggest that the viscosity increases as the mass concentration decreases; this is offered as a potential (although not demonstrated) explanation for the substantially larger viscosities in Zhang et al. and in Renbaum-Wolff et al. The Zhang et al. measurements are still at SOA concentrations above ambient. Isn't it possible that the viscosity of SOA at ambient concentrations is even higher than that reported in Zhang et al.? Or, doesn't it suggest that the "sensitivity" case is actually the better base case, since the concentrations in Zhang et al. are closer to ambient than in Grayson et al.? Overall, I have substantial concerns that the authors are under-emphasizing the potential uncertainty in their estimates in a manner that may influence their conclusions. I think that these issues need to be explored further before this work should be published.

[A14] *To address the referee's comments we have added a section to the revised manuscript that discusses the effect of mass concentration used to generate the SOA on viscosity. See Section 3.5 in the revised manuscript.*

[15] Fig. 2 and Eqn. 4: Regarding the translation between viscosity and mixing time scale, I have some concerns about the authors' illustration. Based on Fig. 2, a viscosity of  $\sim 2e7$  Pa s corresponds to a mixing time scale of 1 h for a 200 nm particle. Using the stated hydrodynamic radius (0.38 nm), the calculated diffusion coefficient for viscosity =  $2e7$  Pa s is  $2.8e-20$  m<sup>2</sup>/s and the mixing timescale for a 200 nm particle is 10 h. Thus, the yellow line in Fig. 2b seems to delineate between  $>10$  h and  $<10$  h, not  $>1$  h and  $<1$  h. My assessment seems consistent with the color scale in Fig. 2b. Similarly, the lines in Fig. 3a and 3b are incorrectly labeled: the line labeled  $>> 1$  h is actually for 10 h. This should not materially affect any conclusions, but should be fixed.

[A15] *Yes, this was a mistake. The mistake has been fixed in the revised manuscript.*

[16] The authors choose 0.5 micrograms/m<sup>3</sup> as their dividing line between what to consider and what not to consider. While reasonable, this is nonetheless an arbitrary choice. Therefore, I suggest that it would be useful if the authors were to graph calculated viscosity vs. mass concentration. Is there any sort of trend that can be used to justify this dividing line?

[A16] *We chose a mass concentration of  $0.5 \mu\text{g m}^{-3}$  for filtering because the mass concentration of organic aerosol at the surface was  $> 0.5 \mu\text{g m}^{-3}$  in all but one of the previous field measurements of organic aerosol at remote locations (Spracklen et al. 2011). To address the referee's comment this information has been added to the revised manuscript. Specifically, we have added the following text to Section 3.2:*

*"We chose a mass concentration of  $> 0.5 \mu\text{g m}^{-3}$  for filtering because the mass concentration of total organic aerosol at the surface was  $> 0.5 \mu\text{g m}^{-3}$  in all but one of the previous field measurements of organic aerosol at remote locations (Spracklen et al., 2011)."*

[17] Fig. 5: Do the authors not find it surprising that RH and T are not less variable with altitude within the PBL during the period shown (13:00-15:00 local time)? I typically think of the PBL as “well mixed” with respect to e.g. RH in the afternoon when mixing is vigorous. Is this a result of averaging over many months.

[A17] Fig. 5 was calculated using a dry adiabatic lapse rate and assuming the mixing ratio of water is independent of height in the PBL. In the revised manuscript we have tried to clarify this point in Section S1. Below is the revised relevant text from Section S1.

10 “The vertical profiles of RH were calculated using the average afternoon surface RHs mentioned above, the vertical profiles of temperature (calculated with the dry adiabatic lapse rate), and assuming the mixing ratio of water is independent of height in the PBL. For the calculations of RH as a function of altitude, the water vapor pressure and water saturated vapour pressure were needed as a function of altitude. The water vapor  
15 pressure as a function of altitude was determined by multiplying the mixing ratio of water by the atmospheric pressure, calculated using the following equation (Seinfeld and Pandis, 2006):”

## Mixing times of organic molecules within secondary organic 20 aerosol particles: a global planetary boundary layer perspective

Adrian M. Maclean<sup>1</sup>, Christopher L. Butenhoff<sup>2</sup>, James W. Grayson<sup>1</sup>, Kelley Barsanti<sup>3</sup>, Jose L. Jimenez<sup>4\*</sup>, Allan K. Bertram<sup>1\*</sup>

<sup>1</sup>Department of Chemistry, University of British Columbia, Vancouver, BC, V6T 1Z1, Canada

25 <sup>2</sup>Dept. of Physics, Portland State University, Portland, Oregon

<sup>3</sup>Department of Chemical and Environmental Engineering and Center for Environmental Research and Technology, University of California, Riverside

<sup>4</sup>Cooperative Institute for Research in the Environmental Sciences and Department of Chemistry and Biochemistry, University of Colorado, Boulder, CO, USA

30

\*To whom correspondence should be addressed. Allan K. Bertram (email): bertram@chem.ubc.ca and Jose L. Jimenez (email): jose.jimenez@colorado.edu

### Abstract

When simulating the formation and life cycle of secondary organic aerosol (SOA) with chemical transport models, it  
35 is often assumed that organic molecules are well mixed within SOA particles on the time scale of 1 h. While this assumption has been debated vigorously in the literature, the issue remains unresolved in part due to a lack of information on the mixing times within SOA particles as a function of both temperature and relative humidity. Using laboratory data, meteorological fields, and a chemical transport model, we ~~determine-estimated~~ how often mixing times are < 1 h within biogenic-SOA in the planetary boundary layer (PBL), the region of the atmosphere where SOA

concentrations are on average the highest). First, a parameterization for viscosity as a function of temperature and RH was developed for  $\alpha$ -pinene SOA using room-temperature and low-temperature viscosity data for  $\alpha$ -pinene SOA generated in the laboratory using mass concentrations of  $\sim 1000 \mu\text{g m}^{-3}$ . Based on this parameterization, the mixing times within  $\alpha$ -pinene SOA are  $< 1$  h for 98.5 % and 99.9 % of the occurrences in the PBL during January and July, respectively, when concentrations are significant (total organic aerosol concentrations are  $> 0.5 \mu\text{g m}^{-3}$  at the surface). Next, as a starting point to quantify how often mixing times of organic molecules are  $< 1$  h within  $\alpha$ -pinene SOA generated using low mass concentrations, we developed a temperature-independent parameterization for viscosity using the room-temperature viscosity data for  $\alpha$ -pinene SOA generated in the laboratory using a mass concentration of  $\sim 70 \mu\text{g m}^{-3}$ . Based on this temperature-independent parameterization, mixing times within  $\alpha$ -pinene SOA are  $< 1$  h for 45 and 38 % of the occurrences in the PBL during January and July, respectively, when concentrations are significant. Finally, a parameterization for viscosity of anthropogenic SOA as a function of temperature and RH was developed using sucrose-water data. Based on this parameterization, and assuming sucrose is a good proxy for anthropogenic SOA, 70 % and 83 % of the mixing times within anthropogenic SOA in the PBL are  $< 1$  h for January and July, respectively, when concentrations are significant. These percentages are likely lower limits due to the assumptions used to calculate mixing times.

Based on laboratory viscosity measurements  $5201400 \mu\text{g m}^{-3}$ , we show that the mixing times are  $< 1$  h most of the time ( $\geq 94$ – $98$  % of the occurrences) when the SOA concentrations are significant  $> 0.5 \mu\text{g m}^{-3}$ . In addition, we show that a reasonable upper limit to the mixing time for most locations is 30 min. Additional measurements are needed to explore further the effect of oxidation level, oxidation type, and gas phase precursor on the viscosity and diffusion within biogenic SOA; nevertheless, based on the available laboratory data, the assumption of well-mixed SOA in chemical transport models seems reasonable for biogenic SOA in most locations in the planetary boundary layer. On the other hand, slow diffusion in biogenic SOA may still be important in the PBL for heterogeneous chemistry. Slow diffusion in biogenic SOA will also be more important in the free troposphere where both the temperature and RH are lower than in the PBL. Mixing times within anthropogenic SOA can be longer than mixing times within biogenic SOA, at least a room temperature, but additional studies of viscosities or diffusion rates of organic molecules within anthropogenic SOA as a function of both temperature and RH are needed to better constrain how often mixing times are  $> 1$  h within anthropogenic SOA in the PBL.

## 1. Introduction

Secondary organic aerosol (SOA) is formed in the atmosphere when volatile organic compounds from biogenic and anthropogenic sources are oxidized by a complex series of reactions to form semivolatile organic compounds (SVOCs), followed by condensation of the lowest volatility products or reactions of the SVOCs dissolved in the particle phase (Ervens et al., 2011; Hallquist et al., 2009). The term “secondary” indicates the aerosol is formed in the atmosphere rather than emitted directly into the atmosphere in the particle phase. Globally, SOA from biogenic sources dominate, with SOA from anthropogenic sources contributing approximately 10 % to the total SOA budget (Hallquist et al., 2009; Spracklen et al., 2011). Major contributors to biogenic SOA are oxidation products of

$\alpha$ -pinene and isoprene (Hu et al., 2015; Kanakidou et al., 2005; Pathak et al., 2007), and as a result, SOA derived from  $\alpha$ -pinene and isoprene are the most widely used representatives of biogenic SOA in experimental and modelling studies.

The planetary boundary layer (PBL) is the lowest part of the atmosphere, ranging from the Earth's surface to roughly 1 km in altitude, depending on location and time (Wallace and Hobbs, 2006). Within this region vertical mixing of air masses is rapid, and on the order of 30 minutes (Wallace and Hobbs, 2006). In addition, within the PBL the temperature varies from roughly 265 K to 305 K and the relative humidity (RH) varies from roughly 20 % to 100 % (see below). SOA concentrations are also on average highest in the PBL (Heald et al., 2011; Wagner et al., 2015).

When simulating the formation, growth, and evaporation of SOA particles with chemical transport models, it is often assumed that SVOCs are well mixed within SOA particles on the time scale of 1 h (Hallquist et al., 2009). If SVOCs are not well mixed within SOA particles on this time scale, then chemical transport models could incorrectly predict SOA mass concentrations by up to an order of magnitude (Shiraiwa and Seinfeld, 2012) and incorrectly predict the size of SOA particles (Zaveri et al., 2014), with implications for air quality and climate predictions (Seinfeld and Pandis, 2006). Recent research has shown that mixing times of organic molecules within SOA particles can be > 1 h at room-temperature and low RHs (Abramson et al., 2013; Grayson et al., 2016; Liu et al., 2016; Perraud et al., 2012; Renbaum-Wolff et al., 2013; Song et al., 2016; Ye et al., 2016; Zhang et al., 2015). In addition, studies have shown that proxies of SOA particles can form glasses at low RHs and low-temperatures (Koop et al., 2011; Zobrist et al., 2008). Nevertheless, the conditions that lead to slow mixing times in SOA may be infrequent on a global scale in the PBL. If this is the case, then the assumption of well mixed SOA particles in chemical transport models should be reasonable. How often mixing times are > 1 h under ambient conditions in the PBL is not well constrained, in part due to the lack of information on mixing times of organic molecules in SOA particles as a function of both RH and temperature.

In the following, we have a) developed a parameterization for the viscosity of  $\alpha$ -pinene SOA particles as a function of both RH and temperature, b) and determined the distribution of RH and temperature in the PBL from an archive of meteorological fields, c) determined the conditions in the PBL when SOA concentrations are significant using a chemical transport model, and d) We then used quantified how this combined information to quantify how often mixing times of SVOCs are > 1 h within  $\alpha$ -pinene and isoprene SOA for ambient temperatures and relative humidities RHs in the for ambient conditions in the PBL. In addition, consider the effect of mass loading on the mixing times and develop a mixing time parameterization for low mass loadings. Mixing times within anthropogenic SOA and the effect of SOA mass concentration on mixing times are also discussed. Our study is complementary to the recent study by Shiraiwa et al. (2017) on the global distribution of particle phase state in atmospheric SOA, although our study focuses on mixing times within SOA in the PBL and uses a different approach to determine physicochemical properties of SOA.

Formatted: Highlight

## 2. Materials and Methods

### 2.1 Parameterization for the viscosity of $\alpha$ -pinene SOA as a function of temperature and RH.

The following data was used to develop a parameterization of the viscosity  $\alpha$ -pinene SOA as a function of temperature and RH: a) room-temperature measurements of viscosity of SOA derived from  $\alpha$ -pinene ozonolysis by Grayson et al. (Grayson et al., 2016) (Table S1), b) low-temperature measurements of viscosity for SOA derived from  $\alpha$ -pinene ozonolysis by Järvinen et al. (Järvinen et al., 2016) (Table S22), and c) temperature dependent measurements of viscosity for water from Crittenden et al. (Crittenden et al., 2012) (Table S33). Järvinen et al. (2016) measured the temperature and RH values at which  $\alpha$ -pinene SOA has a viscosity of approximately  $10^7$  Pa s. In these experiments, SOA was generated with a mass concentration of 707-1414  $\mu\text{g m}^{-3}$ . Grayson et al. (2016) measured viscosity of  $\alpha$ -pinene SOA as a function of RH at 295 K. In these experiments, the SOA was generated with mass concentrations of 121  $\mu\text{g m}^{-3}$  and 520  $\mu\text{g m}^{-3}$ . We use the viscosity measurements from Grayson et al. (2016) determined with a mass concentration of 520  $\mu\text{g m}^{-3}$  to be more consistent with the mass concentrations used by Järvinen et al. (2016). Although there are other room-temperature measurements of the viscosity of  $\alpha$ -pinene SOA (Bateman et al., 2015; Hosny et al., 2016; Kidd et al., 2014; Pajunoja et al., 2014; Renbaum-Wolff et al., 2013), we used the room-temperature measurements from Grayson et al. (2016) because 1) viscosity was measured over a range of relative humidities in this study, 2) the mass concentrations used by Grayson et al. (2016) to generate the SOA were similar to the mass concentrations used by Järvinen et al. (2016), and 3) Grayson et al. (2016) measured the viscosity of the total SOA (both the water soluble component and the water insoluble component).

Due to the experimental conditions used by Grayson et al. (2016) and Järvinen et al. (2016), the parameterization developed here is applicable to SOA generated using a mass concentration of  $\sim 1000 \mu\text{g m}^{-3}$ . We focused on  $\sim 1000 \mu\text{g m}^{-3}$  because both low-temperature and room-temperature viscosity measurements have been carried out using this mass concentration. The effect of mass concentration on the viscosity  $\alpha$ -pinene SOA is discussed in Section 3.5. (Bateman et al., 2015; Hosny et al., 2016; Kidd et al., 2014; Pajunoja et al., 2014; Renbaum-Wolff et al., 2013)

(Bateman et al., 2015) (Grayson et al., 2016) (Zhang et al., 2015) RH (Bateman et al., 2015) (Grayson et al., 2016) (Zhang et al., 2015)  $80-220 \mu\text{g m}^{-3}$   $520 \mu\text{g m}^{-3}$   $70 \mu\text{g m}^{-3}$  (Järvinen et al., 2016)  $700-1400 \mu\text{g m}^{-3}$  Grayson et al. (Grayson et al., 2016) measured viscosities of  $\alpha$ -pinene SOA at two different mass loadings and found the SOA generated at the lower mass loading had a higher viscosity. (Grayson et al., 2016)  $520 \mu\text{g m}^{-3}$  Järvinen (2016)  $520 \mu\text{g m}^{-3}$  by Järvinen et al. (2016). 3.5 (2016) Järvinen (2016). (The viscosity of liquid water as a function of temperature (Crittenden et al., 2012) have parameterization also been measured (Table S3). Recently researchers have measured the viscosity of  $\alpha$ -pinene SOA at room temperature (Bateman et al., 2015; Grayson et al., 2016; Zhang et al., 2015) (Table S1) and low temperatures (Table S2) at various RHs. The viscosity of liquid water as a function of temperature have also been measured (Table S3).) To develop a parameterization for viscosity within  $\alpha$ -pinene SOA as function of temperature and RH, the following equation was fit to these the measurements by Grayson et al. (Grayson et al., 2016), and

Formatted: Font: 10 pt

Field Code Changed

Formatted: Font: 10 pt

Field Code Changed

Formatted: Font: 10 pt

Formatted: Font: 10 pt

Formatted: Font: 10 pt

Field Code Changed

Formatted: Font: 10 pt

Formatted: Font: 10 pt

Formatted: Font: 10 pt

Formatted: Not Highlight



As mentioned above, room-temperature viscosities of  $\alpha$ -pinene SOA as a function of RH were taken from Bateman et al. (2015), Grayson et al. (2016), and Zhang et al. (2015). We have not included the room temperature results from Renbaum-Wolff et al. (2013) or Hosny et al. (2016) since they only measured the viscosity of the water-soluble component of SOA, while the other studies measured the viscosity of the total SOA (water-soluble and water-insoluble component). In addition, we have not used the estimates of viscosity from Kidd et al. (2014) for  $\alpha$ -pinene SOA since the uncertainties in their estimates were too large to help constrain our parameterization. The viscosities reported by Bateman et al. (2015), Grayson et al. (2016) and Zhang et al. (2015) are not inconsistent with most viscosities inferred from diffusion rates within  $\alpha$ -pinene SOA (see Fig. S3 in Grayson et al. (2016)) (Abramson et al., 2013; Cappa and Wilson, 2011; Perraud et al., 2012; Robinson et al., 2013; Saleh et al., 2013).

## 10 2.2. Organic aerosol concentrations in the planetary boundary layer

To determine the conditions in the PBL when SOA concentrations are significant we used the global chemical transport model GEOS-Chem (<http://acmg.seas.harvard.edu/geos/>). The version of GEOS-Chem used (v10-01) includes organic aerosol (OA) formation from semi-volatile and intermediate volatility organic compounds (SVOC and IVOC) (Pye and Seinfeld, 2010), plus new aerosol production from nitrate radical oxidation of isoprene and terpenes and NO<sub>x</sub>-dependent aerosol yields from terpenes (Pye et al., 2010). In this version IVOC emissions are spatially distributed based on naphthalene. To estimate SVOC emissions we scaled the default GEOS-Chem primary organic aerosol (POA) emissions inventory by 1.27 following Pye and Seinfeld (2010). GEOS-Chem was run at a horizontal grid resolution of 4° latitude by 4.5° longitude using GEOS-5 meteorology with 47 vertical layers with a 3-year spin-up period. Shown in Fig. 1 are the monthly averaged total organic aerosol concentrations at the surface for the months of January and July 2006. These monthly averaged total organic aerosol concentrations were used to remove times and locations where SOA concentrations are not expected to be of major importance for climate, health or visibility.

## 2.3 RH and temperature in the PBL

Information on the RH and temperature distributions in the global PBL in different seasons ~~are were~~ also needed to assess mixing times within SOA particles. ~~First, the afternoon PBL heights were determined globally using the 6-h averaged GEOS-5 meteorology fields. Then, temperature and RH in each grid cell within the PBL were determined globally using the 6-h averaged GEOS-5 meteorology fields. To determine if a grid cell was within the PBL, the afternoon PBL heights mentioned above were used, and PBL heights. To determine if a grid cell was within the PBL, these PBL heights were used.~~ The GEOS-5 archive provides temperature and RH at a horizontal grid resolution of 4° latitude by 4.5° longitude and 47 vertical layers. ~~Shown in Fig 2 are the temperature and RH conditions at the Earth's surface for January and July. The conditions for the top of the planetary boundary layer can be found in Fig. S1.~~

### 3. Results and Discussion

#### 3.1 Parameterization of viscosity and mixing times within $\alpha$ -pinene SOA particles as a function of RH and temperature.

Shown in Fig. 2a (contours) is the RH and temperature dependent parameterization for  $\alpha$ -pinene SOA viscosities based on the viscosities measured at room-temperature (Grayson et al., 2016) and low-temperature (Järvinen et al., 2016), as well as the viscosity of water as a function of temperature (Crittenden et al., 2012). From the viscosity parameterization, the diffusion coefficients of organic molecules within  $\alpha$ -pinene SOA particles were calculated using the Stokes-Einstein equation:

$$D = \frac{kT}{6\pi\eta R_H} \quad (35)$$

where  $D$  is the diffusion coefficient,  $k$  is the Boltzmann constant,  $T$  is temperature in Kelvin,  $\eta$  is the dynamic viscosity and  $R_H$  is the hydrodynamic radius of the diffusing species. For the calculations, a hydrodynamic radius of 0.38 nm was used for the diffusing organic molecules within SOA, based on an assumed molecular weight of 175 g mol<sup>-1</sup> (Huff Hartz et al., 2005), a density of 1.3 g cm<sup>-3</sup> (Chen and Hopke, 2009; Saathoff et al., 2009) and spherical symmetry. The Stokes-Einstein equation should give reasonable values when the radius of the diffusing molecules is roughly greater than or equal to the same size as the radius of the matrix molecules and when the viscosity of the matrix is relatively small ( $\lesssim 400$  Pa s) (Chenyakin et al., 2017; Price et al., 2016). When the viscosity of the matrix is large ( $\gtrsim 10^6$  Pa s), the Stokes-Einstein equation can under-predict diffusion coefficients of organic molecules in organic matrices (Champion et al., 1997; Chenyakin et al., 2017; Price et al., 2016). Hence, the diffusion coefficients and mixing times estimated here should be considered lower and upper limits, respectively.

From the diffusion coefficients, the mixing times of organic molecules within an  $\alpha$ -pinene SOA particle were calculated with the following equation (Shiraiwa et al., 2011):

$$\tau_{mix} = \frac{d^2}{4\pi^2 D} \quad (46)$$

where  $\tau_{mix}$  is the mixing time,  $d$  is the diameter of an SOA particle, and  $D$  is the diffusion coefficient estimated from Eq. (35). For these calculations, it was assumed that the  $\alpha$ -pinene SOA particles have a diameter of 200 nm, which is roughly the median diameter in the volume distribution of ambient SOA-containing particles (Martin et al., 2010; Pöschl et al., 2010; Riipinen et al., 2011). Once the mixing time has elapsed, the concentration of the diffusing molecules at the centre of the particle is within 1/e of the equilibrium concentration (Shiraiwa et al., 2011). The calculated mixing times (Fig. 2b) illustrate that, as expected, indirect-inverse relationships exist between both mixing time and RH, as well as mixing time and temperature.

#### 3.2 RH and temperature in the PBL

Shown in Figs. 3a and 3b are the normalized frequency counts of temperature and RH in the PBL for the months of January and July, 2006, respectively, based on the archive of meteorological fields (GEOS-5) used in the global chemical transport model, GEOS-Chem, v10-01. We only included grid points in our analysis if the grid points were

within the PBL and the monthly average mass concentration of total organic aerosol was  $> 0.5 \mu\text{g m}^{-3}$  at the surface, based on GEOS-Chem, v10-01 (Fig. 1). In other words, we included all the grid points in a column up to the top of the PBL when determining frequency counts if the monthly averaged total organic aerosol concentration was  $> 0.5 \mu\text{g m}^{-3}$  at the surface. This filtering removes cases where SOA concentrations are not expected to be of major importance

5 for climate, health or visibility. We chose a mass concentration of  $> 0.5 \mu\text{g m}^{-3}$  for filtering because the mass concentration of total organic aerosol at the surface was  $> 0.5 \mu\text{g m}^{-3}$  in all but one of the previous field measurements of organic aerosol at remote locations (Spracklen et al., 2011).

This concentration was chosen as it had been determined by Spracklen et al. (Spracklen et al., 2011) that the majority of surface measurements of organic aerosols, including in remote locations, had concentrations  $> 0.5 \mu\text{g m}^{-3}$ . The normalized frequency counts illustrate that the temperature and RH in the PBL are often in the range of 290-300 K and  $> 50\%$  RH for the month of January (Fig. 33a) and in the range of 285-300 K and  $> 30\%$  RH for the month of July (Fig. 33b). For reference, shown in Figs. S1S1 and S2 are the average temperature and RH conditions at the Earth's surface and top of the planetary boundary layer, respectively, for January and July, based on the archive of meteorological fields for 2006 (GEOS-5).

### 3.3 Mixing times of organic molecules within $\alpha$ -pinene SOA particles in the PBL

Also shown in Figs. 33a and 33b are the contour mixing times within 200 nm  $\alpha$ -pinene SOA particles predicted with our lines produced using our parameterization (contours) of mixing times of organics within 200 nm  $\alpha$ -pinene SOA particles. These results, together with the frequency counts of temperature and RH throughout the vertical column of 20 the PBL, indicate that the mixing times of organic molecules within  $\alpha$ -pinene SOA are often  $< 1 \times 10^{-1}$  h for conditions in the PBL.

Shown in Fig. 44 are the normalized frequency distributions of mixing times within  $\alpha$ -pinene SOA for January and July, based on the data in Figs. 33a and 33b. Figure 44 suggests that the mixing times within  $\alpha$ -pinene SOA are  $< 1$  h for 94-98.5% and 99.9% of the occurrences in the PBL during January and July, respectively, when monthly average total organic aerosol concentrations are  $> 0.5 \mu\text{g m}^{-3}$  at the surface. Takegawa et al. (Takegawa et al., 2006) found that aged aerosol particles can have diameters larger than 200 nm, so the mixing time calculations were repeated for a particle size of 500 nm (Figure S2). It was found that the mixing times with the 500 nm particles was  $< 1$  h for 95.9% and 99.4% of the occurrences in the PBL during January and July, respectively.

Within the PBL, RH increases and temperature decreases with altitude, with both changes being substantial and 30 impacting mixing times in opposite directions. Shown in Fig. 55a-c are calculated monthly average afternoon (13:00-15:00, local time) vertical profiles of temperature, RH, and mixing times within  $\alpha$ -pinene SOA over Hyytiälä (boreal forest), and the Amazon (rainforest) for the driest month of the year at each these locations (the method used to calculate vertical profiles is described in the Supporting Information, Section S2S1). Afternoon vertical profiles were chosen since this is the time of the day when RH is typically lowest and thus mixing times are the longest. Figure 5e 35 5e shows that mixing times within  $\alpha$ -pinene SOA decrease significantly with altitude for these two locations. This is because the plasticizing effect of water on viscosity dominates the temperature effect for these conditions.

Formatted: Font: (Default) +Body (Times New Roman)

Formatted: Font: (Default) +Body (Times New Roman),  
Font color: Text 1

Formatted: Font: (Default) +Body (Times New Roman), 10  
pt, Font color: Text 1

Formatted: Font: (Default) +Body (Times New Roman)

Formatted: Font: (Default) +Body (Times New Roman)

Shown in Fig. 66 are global maps of the monthly averaged mixing times of organic molecules within  $\alpha$ -pinene SOA for conditions at the top of the PBL for the months of January and July. Figure 6-6 shows that 83-91.2 % and 92-97.5 % of the locations for January and July, respectively, have a mixing time  $< 0.1$  h for conditions at the top of the PBL when monthly averaged total organic aerosol surface concentrations are  $> 0.5 \mu\text{g m}^{-3}$ . Within the PBL, vertical mixing of air masses occurs on the order of 30 min. Since the mixing times within  $\alpha$ -pinene SOA particles for conditions at the top of the PBL are  $< 0.1$  h for most locations where the SOA concentrations are significant (total organic aerosol concentration  $> 0.5 \mu\text{g m}^{-3}$  at the surface), a reasonable upper limit to the mixing time within the  $\alpha$ -pinene SOA studied here for most locations in the PBL is 30 min. During this 30 min interval, mixing times within  $\alpha$ -pinene SOA particles can cycle between short and long values, though rarely being  $> 1$  h (Figs. 33 and 44).

~~Shiraiwa et al. (Shiraiwa et al., 2017) performed a similar study to investigate the mixing time in SOA particles in the atmosphere. The researchers used the relationship between volatility, molar mass and O:C ratio to predict the glass transition temperature of the SOA. The ratio of the glass transition temperature and the ambient temperature were related to the phase state of the SOA particle and from their mixing times were inferred. The mixing times were determined at several different pressures to study the mixing time at different altitudes. The two studies agree that mixing times are expected to be short in regions such as the Amazon, Europe and at high latitudes and longer mixing times will occur in the western United States as well as the Sahara desert. However, in general, this study predicts shorter mixing times overall than those described in Shiraiwa et al. (Shiraiwa et al., 2017), however this study focuses on one particular type of SOA whereas the study by Shiraiwa et al. (2017) does not focus on one type of SOA.~~

#### 3.4 Sensitivity analysis for $\alpha$ -pinene SOA particles in the PBL

##### 3.4 Sensitivity analysis

To calculate the mixing times discussed above, we assumed that the  $\alpha$ -pinene SOA particles have a diameter of 200 nm. We also repeated these calculations assuming a diameter of 500 nm, since aged organic aerosol can have larger diameters, however, a (Takegawa et al., 2006). Based on the viscosity parameterization shown in Fig. 2a, mixing times within 500 nm  $\alpha$ -pinene SOA particles are  $< 1$  h for 95.9 % and 99.4 % of the occurrences in the PBL during January and July, respectively (Fig. S23).

The parameterization for the viscosity used for  $\alpha$ -pinene SOA was above was developed using based on viscosity measurements from by Bateman et al. (2015), Grayson et al. (2016), Zhang et al. (2015), Järvinen et al. (2016) and Crittenden et al. (2012). As a sensitivity analysis, we developed a second parameterization, using the same procedure as describe above, but using the upper limits to the viscosities reported by Grayson et al. (2016) and the upper limits to the RH ranges reported by Järvinen et al. (2016). This should result in an upper limit to the viscosity parameterization discussed above. The (Grayson et al., 2016) (Järvinen et al., 2016) uncertainties in the measurements by Crittenden et al. (Crittenden et al., 2012) were not considered since they are small compared to the uncertainties reported by Grayson et al. (2016) and Järvinen et al. (2016). The viscosity measurements reported by Grayson et al. (Grayson et al., 2016) covered roughly 1-2 orders of magnitude at each RH, as well the values reported by Järvinen et al. (Järvinen et al., 2016) at each temperature covered a RH range of 5-10%. As a sensitivity analysis, we developed two additional parameterizations, using the same procedure as above. The first parameterization used

Formatted: Heading 2

Formatted: Heading 2

the lower viscosity values reported by Grayson et al. (Grayson et al., 2016) and the lower RH reported by Järvinen et al. (Järvinen et al., 2016), and the second parameterization used the upper viscosity and RH limits of Grayson et al. (Grayson et al., 2016) and upper Järvinen et al. (Järvinen et al., 2016), respectively. The frequency of the mixing times for January and July for both parameterizations are shown in Figures S3 and S4, respectively. For the upper limits based on this second parameterization, mixing times are < 1 h for 96.6 % and 99.5 % of the occurrences in the PBL during January and July, respectively, when the total organic aerosol was > 0.5  $\mu\text{g m}^{-3}$  at the surface (Fig. S34). For January, 96.6% of the conditions in the PBL resulted in mixing times < 1 hr (previously 98.5%) and for July, 99.5% of the conditions resulted in mixing times < 1 hr (previously 99.9%) when the total organic aerosol was > 0.5  $\mu\text{g m}^{-3}$  at the surface. None of these results impact the overall conclusions of the paper. The measurements by Zhang et al. (2015) and Grayson et al. (2016) were both carried out at room temperature and over a similar range in RH. The viscosities reported by Zhang et al. (2015) were higher than the viscosities reported by Grayson et al. (2016) (see Table S1). As a sensitivity analysis, we developed a second parameterization, using the same procedure as described above, but excluding the data from Grayson et al. (2016) in the fitting procedure. Based on this new parameterization, for January, 86 % of the conditions in the PBL resulting in mixing times < 1 h (previously 93 %) and for July, 96 % of the conditions producing mixing times < 1 h (previously 98 %) when the total organic aerosol was > 0.5  $\mu\text{g m}^{-3}$  at the surface. Using this new parameterization, we also found that the number of locations with mixing times < 0.1 h decreased from 83 to 80 % and 92 to 89 % for January and July, respectively. None of these results significantly impact the overall conclusions of the paper.

### 3.5 Effect of mass concentration used to generate the SOA

The parameterizations developed above were based on SOA generated using a mass concentration of ~ 1000  $\mu\text{g m}^{-3}$ . As mentioned, we focused on ~ 1000  $\mu\text{g m}^{-3}$  because low-temperature and room-temperature viscosity measurements have been carried out using this mass concentration. However, the viscosity of some types of SOA may depend on the mass concentration used to generate the SOA. For example, results from Grayson et al. (Grayson et al., 2016) showed that under dry conditions, the viscosity of  $\alpha$ -pinene SOA may increase by a factor of 5 as the production mass concentration decreased from 1200  $\mu\text{g m}^{-3}$  to 120  $\mu\text{g m}^{-3}$ . In addition, mass concentrations of biogenic SOA are typically < 10  $\mu\text{g m}^{-3}$  in the atmosphere (Spracklen et al., 2011). indicate that SOA generated at low mass loading has higher viscosities than SOA generated at high mass loadings. As a starting point to quantify how often mixing times of organic molecules are < 1 h within  $\alpha$ -pinene SOA generated using low mass concentrations, we developed a temperature-independent parameterization using the upper limit of the room-temperature viscosity data for  $\alpha$ -pinene SOA from Zhang et al. (Zhang et al., 2015) (Table SX5) and room-temperature viscosity data for water from (Crittenden et al., 2012) (Table SY3). Zhang et al. (2015) measured the viscosity of  $\alpha$ -pinene SOA over a range of relative humidities (0–60 %), and the SOA used in these experiments was generated in the laboratory using a mass concentration of ~ 70  $\mu\text{g m}^{-3}$ . The median room-temperature viscosities reported by Zhang et al. are higher than the median room-temperature viscosities reported by Grayson et al. (2016) using a mass concentration of 520  $\mu\text{g m}^{-3}$  (Fig. SX5). Although not proven, a reasonable explanation for the difference in median viscosities is the difference in mass concentrations used to generate the SOA.

Formatted: Font color: Red

Formatted: Heading 2

Formatted: Don't adjust space between Latin and Asian text, Don't adjust space between Asian text and numbers

$70 \mu\text{g m}^{-3}$  (Crittenden et al., 2012). A temperature-independent parameterization was generated by fitting Eq. (1) to the upper limit of the room-temperature viscosity data from Zhang et al. (Zhang et al., 2015) and water viscosity from Crittenden et al. (Crittenden et al., 2012), but with the temperature (T) in Eq. (1) replaced by 293 K. The values for the parameters retrieved by fitting the modified Eq. (1) to the viscosity data are reported in Table S6. The temperature-independent parameterization generated using this method is shown in Figure S7a. Shown in Figs. 7b, 8a, and 8b (contours) is the parameterization for the viscosity and mixing times within 200 nm  $\alpha$ -pinene SOA based on this temperature-independent viscosity parameterization. Also included in Figs. 8a and 8b are the normalized frequency counts of temperature and RH in the PBL for the months of January and July, 2006, respectively, when the monthly average mass concentration of total organic aerosol was  $> 0.5 \mu\text{g m}^{-3}$  at the surface. Shown in Fig. 9 are the normalized frequency distributions of mixing times within  $\alpha$ -pinene SOA for January and July, based on the data in Figs. 8a and 8b. Figure 9 suggests that the mixing times within  $\alpha$ -pinene SOA is  $< 1$  h for 45 and 38 % of the occurrences in the PBL during January and July, respectively, when monthly average total organic aerosol concentrations were  $> 0.5 \mu\text{g m}^{-3}$  at the surface. The frequency of the different conditions and the expected mixing times and the frequency of the different mixing times can be seen in Figures S6 and S7, respectively. However, several caveats need to be emphasized: 1) the parameterization was developed based on room-temperature viscosity data only. Viscosities, and hence mixing times, will increase as temperature decreases. As an illustration, the viscosity of sucrose-water mixtures can increase by 2-3 orders of magnitude as the temperature decreases by 10 K close to the glass transition temperature (Champion et al., 1997). 2) The mixing times were calculated using the Stokes-Einstein relation, which can underpredict diffusion coefficients, and hence overpredict mixing times, when the viscosity of the matrix is high. —For example, the Stokes-Einstein equation can underpredict diffusion coefficients of organic molecules in sucrose-water mixtures by at least a factor of 10 to 100 at viscosities  $\geq 10^6$  Pa s (Chenyakin et al., 2017; Price et al., 2016). 3) The viscosity data from Zhang et al. (Zhang et al., 2015) has an uncertainty of  $\pm 1$  order of magnitude, which was not considered in the temperature-independent parameterization. Considering these caveats, we are unable to make strong conclusions about how often mixing times of organic molecules are  $< 1$  h within  $\alpha$ -pinene SOA generated at low mass concentrations. To help resolve this issue, temperature dependent studies of the viscosity of  $\alpha$ -pinene SOA generated using low mass concentrations are needed. Also, the accuracy of the Stokes-Einstein equation for predicting diffusion coefficients of organics within  $\alpha$ -pinene SOA needs to be determined. (since the upper limit of the viscosity was used)

### 3.65 Mixing times of organic molecules within isoprene SOA particles in the PBL

The discussion in sections 3.1–3.4.5 is based on SOA generated from the ozonolysis of  $\alpha$ -pinene. Another major global source of SOA is photo oxidation of biogenic isoprene (Hallquist et al., 2009; Hu et al., 2015). The viscosity of isoprene SOA is lower than the viscosity of  $\alpha$ -pinene SOA at room temperature (Song et al., 2015). As a result, the conclusions reached above for  $\alpha$ -pinene SOA are likely applicable to isoprene SOA as well.

A caveat to the discussion above is that the measurements of viscosities used to generate the parameterization shown in Fig. 32a were carried out on SOA samples generated with mass concentrations of  $\geq 70 \mu\text{g m}^{-3}$ , which is higher than the concentrations of biogenic SOA in the atmosphere. Additional studies of the viscosity of  $\alpha$ -pinene SOA generated using lower mass loadings are needed. Additional studies are also needed to further explore the effect of oxidation level (Ng et al., 2010), oxidant type (Pajunoja et al., 2014), and the presence of water during oxidation on the viscosity of biogenic SOA (Kidd et al., 2014). Studies are also needed to investigate the viscosity of other types of biogenic SOA (Kanakidou et al., 2005). Additional studies of the viscosity of  $\alpha$ -pinene SOA generated at lower mass loadings are needed. Nevertheless, based on the data available it is not clear that long mixing times of SVOCs need to be included in chemical transport models when simulating SOA from biogenic sources in the global PBL.

Despite the discussion above, it is important to keep in mind that slow diffusion in biogenic SOA is likely still important in the atmosphere for other reasons. For example, slow diffusion is likely to be important for heterogeneous chemistry within biogenic SOA in the PBL (Shiraiwa et al., 2011). Slow diffusion is also likely important when simulating the partitioning of SVOCs into biogenic SOA in the free troposphere where both the temperature and RH are lower than in the PBL (Shiraiwa et al., 2017).

### 3.66 Mixing times of organic molecules within anthropogenic SOA particles in the PBL

Recently it has been shown that the diffusion rates of organics in SOA from toluene photooxidation are slower than the diffusion rates of organics in SOA from  $\alpha$ -pinene ozonolysis and isoprene photooxidation at room-temperature (Liu et al., 2016; Song et al., 2016; Ye et al., 2016). These results indicate that mixing times are longer in some types of anthropogenic SOA than some types of biogenic SOA, at least at room-temperature. SOA derived from anthropogenic sources can be a significant contributor to SOA over polluted regions (Hallquist et al., 2009; Spracklen et al., 2011). Viscosities or diffusion rates within toluene SOA or other types of anthropogenic SOA have yet to be measured at temperatures lower than room-temperature. As a result, we have used sucrose as a proxy of anthropogenic SOA, since the viscosity of sucrose is similar to the viscosity of toluene SOA at room-temperature (Fig. S4S6) (Power and Reid, 2014; Song et al., 2016), and since a parameterization of the viscosity of sucrose as a function of temperature and RH can be developed using literature data. In the Supporting Information (Section S3S2, Table S5S7-S7S9, and Fig. S2S7-S5S10) we carried out a similar analysis for sucrose as for  $\alpha$ -pinene SOA above. Assuming sucrose is a good proxy for anthropogenic SOA, the analysis suggests that 70 % and 83 % of the mixing times within anthropogenic SOA in the PBL are  $< 1$  h for January and July, respectively, when SOA concentrations are significant (total organic aerosol concentration  $> 0.5 \mu\text{g m}^{-3}$  at the surface). In addition, 81 % and 87 % of the locations for January and July, respectively, have a mixing time  $< 0.1$  h at the top of the PBL when surface concentrations of total organic aerosol are  $> 0.5 \mu\text{g m}^{-3}$ . These percentages for anthropogenic SOA are likely lower limits since, as mentioned earlier, studies have shown that the Stokes-Einstein relation (which is used here to calculate diffusion coefficients of organic molecules from viscosities) can under-predict diffusion coefficients of organic molecules in sucrose-water mixtures by at least a factor of 10 to 100 at viscosities  $\geq 10^6$  Pa s (Chenyakin et al., 2017; Price et al., 2016). Measurements of diffusion rates of organic molecules within anthropogenic SOA as a function of

both temperature and RH are needed to better constrain how often mixing times are > 1 h within anthropogenic SOA in the PBL.

### 3.3.87. Comparison with previous studies

5 ~~Our study is complementary to the recent study by Shiraiwa et al. (2017) recently estimated mixing times of organics within SOA in the troposphere using a global chemistry climate model and a relationship between glass transition temperatures, molar mass, and oxygen-to-carbon elemental ratios. on~~ Their results suggest mixing times of organics within SOA are short (< 1 min) over the oceans, tropics, and high latitudes at the surface and 850 hPa. On the other hand, their results suggest mixing times are long (> 1 hour) over dry regions (i.e. major deserts) at the surface and at  
10 850 hPa and over most continental regions at 850 hPa. The general trends observed by Shiraiwa et al. (2017) are consistent with the trends observed here. However, the mixing times predicted by Shiraiwa et al. (2017) appear to be longer~~shorter~~ than the mixing times predicted here using viscosities of  $\alpha$ -pinene SOA generated with a mass concentration  $\sim 1000 \mu\text{g m}^{-3}$ . Quantitative differences between the current work and the work by Shiraiwa et al. (2017) ~~are~~is not surprising since Shiraiwa et al. (2017) considered both anthropogenic SOA and biogenic SOA  
15 simultaneously, and since they used a very different approach to estimate viscosities of atmospheric SOA.~~the global distribution of particle phase state in atmospheric SOA, although our study focuses on mixing times within SOA in the PBL and uses a different approach to determine physicochemical properties of SOA.~~

Formatted: Font color: Auto

Formatted: Font color: Auto

Formatted: Heading 2

Formatted: Font color: Auto

### 20 4.0 Summary and Conclusions

~~We report the expected atmospheric mixing times in  $\alpha$ -pinene SOA for atmospheric temperature and RH data, based on a parameterization developed using laboratory viscosity data of high mass loading SOA ( $520-1400 \mu\text{g m}^{-3}$ ). A parameterization for viscosity as a function of temperature and RH was developed for  $\alpha$ -pinene SOA based on room-  
25 temperature and low-temperature viscosity data of  $\alpha$ -pinene SOA generated in the laboratory using mass concentrations of  $\sim 1000 \mu\text{g m}^{-3}$ . We focused on  $\sim 1000 \mu\text{g m}^{-3}$  because low-temperature and room-temperature viscosity measurements have been carried out using this mass concentration. Based on this parameterization, as well as RH and temperatures in the PBL, the mixing times within  $\alpha$ -pinene SOA ~~are~~is < 1 h for 98.5 % and 99.9 % of the occurrences in the PBL during January and July, respectively, when monthly average total organic aerosol  
30 concentrations ~~are~~were >  $0.5 \mu\text{g m}^{-3}$  at the surface. It was determined that 98.5% and 99.9% of locations with significant SOA concentrations, for January and July respectively, will have rapid mixing times. Also based on this parameterization, 91.2 % and 97.5 % of the locations for January and July, respectively, have a mixing time < 0.1 h for conditions at the top of the PBL when monthly averaged total organic aerosol surface concentrations are >  $0.5 \mu\text{g m}^{-3}$ .~~

Formatted: Font: Bold, Font color: Auto

Formatted: Heading 2

As a starting point to quantify how often mixing times of organic molecules are < 1 h within  $\alpha$ -pinene SOA generated using low mass concentrations, we developed a temperature-independent parameterization using the room-temperature viscosity data for  $\alpha$ -pinene SOA from Zhang et al. (2015). Zhang et al. (2015) measured the viscosity of  $\alpha$ -pinene SOA generated using a mass concentration of  $\sim 70 \mu\text{g m}^{-3}$ . Based on this temperature-independent parameterization, mixing times within  $\alpha$ -pinene SOA are < 1 h for 45 and 38 % of the occurrences in the PBL during January and July, respectively, when monthly average total organic aerosol concentrations are  $> 0.5 \mu\text{g m}^{-3}$  at the surface. However, several caveats need to be emphasized for these results. Most important, the results were based on room-temperature viscosity data only and the mixing times were calculated using the Stokes-Einstein relation, which can underpredict diffusion coefficients of organic molecules, and hence overpredict mixing times, when the viscosity of the matrix is high.

As a starting point to quantify how often mixing times of organic molecules are < 1 h within anthropogenic SOA, a parameterization for viscosity as a function of temperature and RH was developed using sucrose-water viscosity data. Based on this parameterization and assuming sucrose is a good proxy for anthropogenic SOA, 70 % and 83 % of the mixing times within anthropogenic SOA in the PBL are < 1 h for January and July, respectively, when SOA concentrations are significant (total organic aerosol concentration  $> 0.5 \mu\text{g m}^{-3}$  at the surface). These percentages for anthropogenic SOA are likely lower limits since studies have shown that the Stokes-Einstein relation (which is used here to calculate diffusion coefficients of organic molecules from viscosities) can underpredict diffusion coefficients of organic molecules in sucrose-water mixtures by at least a factor of 10 to 100 at viscosities  $\geq 10^6 \text{ Pa s}$  (Chenyakin et al., 2017; Price et al., 2016).

To improve the predictions presented above the following are needed: 1) viscosities as a function of temperature and RH for  $\alpha$ -pinene SOA and anthropogenic SOA generated using low mass concentrations and 2) studies that quantify the accuracy of the Stokes-Einstein equation for predicting diffusion coefficients in SOA. Studies that explore further the effect of oxidation level, oxidation type, and gas-phase precursor on viscosity and diffusion within biogenic and anthropogenic SOA would also be beneficial.

However, measurements have indicated that viscosities, and thus mixing times, increase with decreasing mass loading. We are left to conclude that additional studies are needed to fully understand the impact of mass loading on the viscosity and mixing times in SOA particles. Specific experiments that would be helpful are viscosity measurements at atmospherically relevant mass loadings at room temperature and low temperatures across a range of RHs. As well, diffusion measurements in the SOA particles to determine the break-down of the Stokes-Einstein equation in the high viscosity SOA particles. Additional studies are also needed to further explore the effect of oxidation level (Ng et al., 2010), oxidant type (Pajunoja et al., 2014), and the presence of water during oxidation on the viscosity of biogenic SOA (Kidd et al., 2014). Studies are also needed to investigate the viscosity of other types of biogenic SOA (Kanakidou et al., 2005).

*Competing interests:* The authors declare that they have no conflict of interest.

**Acknowledgments.** This work was funded by the Natural Science and Engineering Research Council of Canada, DOE (ASR/BER) DE-SC0016559 & EPA STAR 83587701-0. This manuscript has not been reviewed by EPA and thus no endorsement should be inferred. Support from the MJ Murdock Charitable Trust (Grant 2012183) for computing infrastructure at Portland State University is acknowledged, as well as assistance from S.J. Hanna with the Amazon temperature and humidity data.

## References

- Abramson, E., Imre, D., Beranek, J., Wilson, J. and Zelenyuk, A.: Experimental determination of chemical diffusion within secondary organic aerosol particles, *Phys. Chem. Chem. Phys.*, 15(8), 2983–2991, doi:10.1039/C2CP44013J, 2013.
- Bateman, A. P., Bertram, A. K. and Martin, S. T.: Hygroscopic Influence on the Semisolid-to-Liquid Transition of Secondary Organic Materials, *J. Phys. Chem. A*, 119(19), 4386–4395, doi:10.1021/jp508521c, 2015.
- Champion, D., Hervet, H., Blond, G., LeMeste, M. and Simatos, D.: Translational diffusion in sucrose solutions in the vicinity of their glass transition temperature, *J. Phys. Chem. B*, 101(50), 10674–10679, doi:10.1021/jp971899i, 1997.
- Chen, X. and Hopke, P. K.: Secondary organic aerosol from  $\alpha$ -pinene ozonolysis in dynamic chamber system, *Indoor Air*, 19(4), 335–345, doi:10.1111/j.1600-0668.2009.00596.x, 2009.
- Chenyakin, Y., Ullmann, D. A., Evoy, E., Renbaum-Wolff, L., Kamal, S. and Bertram, A. K.: Diffusion coefficients of organic molecules in sucrose-water solutions and comparison with Stokes-Einstein predictions, *Atmos. Chem. Phys.*, 17(3), 2423–2435, doi:10.5194/acp-2016-740, 2017.
- Corti, H. R., Frank, G. A. and Marconi, M. C.: An Alternate Solution of Fluorescence Recovery Kinetics after Spot-Bleaching for Measuring Diffusion Coefficients. 2. Diffusion of Fluorescein in Aqueous Sucrose Solutions, *J. Solution Chem.*, 37(11), 1593–1608, doi:10.1007/s10953-008-9329-4, 2008.
- Crittenden, J. C., Trussel, R. R., Hand, D. W., Howe, K. J. and Tchobanoglous, G.: *MWH's Water Treatment*, John Wiley and Sons., 2012.
- Ervens, B., Turpin, B. J. and Weber, R. J.: Secondary organic aerosol formation in cloud droplets and aqueous particles (aqSOA): a review of laboratory, field and model studies, *Atmos. Chem. Phys.*, 11(21), 11069–11102, doi:10.5194/acp-11-11069-2011, 2011.
- Grayson, J. W., Zhang, Y., Mutzel, A., Renbaum-Wolff, L., Boege, O., Kamal, S., Herrmann, H., Martin, S. T. and Bertram, A. K.: Effect of varying experimental conditions on the viscosity of alpha-pinene derived secondary organic material, *Atmos. Chem. Phys.*, 16(10), 6027–6040, doi:10.5194/acp-16-6027-2016, 2016.
- Hallquist, M., Wenger, J. C., Baltensperger, U., Rudich, Y., Simpson, D., Claeys, M., Dommen, J., Donahue, N. M., George, C., Goldstein, A. H., Hamilton, J. F., Herrmann, H., Hoffmann, T., Iinuma, Y., Jang, M., Jenkin, M. E., Jimenez, J. L., Kiendler-Scharr, A., Maenhaut, W., McFiggans, G., Mentel, T. F., Monod, A., Prevot, A. S. H., Seinfeld, J. H., Surratt, J. D., Szmigielski, R. and Wildt, J.: The formation, properties and impact of secondary organic

- aerosol: current and emerging issues, *Atmos. Chem. Phys.*, 9(14), 5155–5236, doi:10.5194/acp-9-5155-2009, 2009.
- Heald, C. L., Coe, H., Jimenez, J. L., Weber, R. J., Bahreini, R., Middlebrook, A. M., Russell, L. M., Jolleys, M., Fu, T. M., Allan, J. D., Bower, K. N., Capes, G., Crosier, J., Morgan, W. T., Robinson, N. H., Williams, P. I., Cubison, M. J., Decarlo, P. F. and Dunlea, E. J.: Exploring the vertical profile of atmospheric organic aerosol: Comparing 17 aircraft field campaigns with a global model, *Atmos. Chem. Phys.*, 11(24), 12676–12696, doi:10.5194/acp-11-12673-2011, 2011.
- Hosny, N. A., Fitzgerald, C., Vyšniauskas, A., Athanasiadis, A., Berkemeier, T., Uygur, N., Pöschl, U., Shiraiwa, M., Kalberer, M., Pope, F. D. and Kuimova, M. K.: Direct imaging of changes in aerosol particle viscosity upon hydration and chemical aging, *Chem. Sci.*, 7(2), 1357–1367, doi:10.1039/C5SC02959G, 2016.
- 10 Hu, W. W., Campuzano-Jost, P., Palm, B. B., Day, D. A., Ortega, A. M., Hayes, P. L., Krechmer, J. E., Chen, Q., Kuwata, M., Liu, Y. J., De Sá, S. S., McKinney, K., Martin, S. T., Hu, M., Budisulistiorini, S. H., Riva, M., Surratt, J. D., St. Clair, J. M., Isaacman-Van Wertz, G., Yee, L. D., Goldstein, A. H., Carbone, S., Brito, J., Artaxo, P., De Gouw, J. A., Koss, A., Wisthaler, A., Mikoviny, T., Karl, T., Kaser, L., Jud, W., Hansel, A., Docherty, K. S., Alexander, M. L., Robinson, N. H., Coe, H., Allan, J. D., Canagaratna, M. R., Paulot, F. and Jimenez, J. L.:
- 15 Characterization of a real-time tracer for isoprene epoxydiols-derived secondary organic aerosol (IEPOX-SOA) from aerosol mass spectrometer measurements, *Atmos. Chem. Phys.*, 15(20), 11807–11833, doi:10.5194/acp-15-11807-2015, 2015.
- Huff Hartz, K. E., Rosenørn, T., Ferchak, S. R., Raymond, T. M., Bilde, M., Donahue, N. M. and Pandis, S. N.: Cloud condensation nuclei activation of monoterpene and sesquiterpene secondary organic aerosol, *J. Geophys. Res. D Atmos.*, 110(14), 1–8, doi:10.1029/2004JD005754, 2005.
- 20 Järvinen, E., Ignatius, K., Nichman, L., Kristensen, T. B., Fuchs, C., Hoyle, C. R., Höppel, N., Corbin, J. C., Craven, J., Duplissy, J., Ehrhart, S., El Haddad, I., Frege, C., Gordon, H., Jokinen, T., Kallinger, P., Kirkby, J., Kiselev, A., Naumann, K. H., Petäjä, T., Pinterich, T., Prevot, A. S. H., Saathoff, H., Schiebel, T., Sengupta, K., Simon, M., Slowik, J. G., Tröstl, J., Virtanen, A., Vochezer, P., Vogt, S., Wagner, A. C., Wagner, R., Williamson, C., Winkler, P. M.,
- 25 Yan, C., Baltensperger, U., Donahue, N. M., Flagan, R. C., Gallagher, M., Hansel, A., Kulmala, M., Stratmann, F., Worsnop, D. R., Möhler, O., Leisner, T. and Schnaiter, M.: Observation of viscosity transition in  $\alpha$ -pinene secondary organic aerosol, *Atmos. Chem. Phys.*, 16(7), 4423–4438, doi:10.5194/acp-16-4423-2016, 2016.
- Kanakidou, M., Seinfeld, J. H., Pandis, S. N., Barnes, I., Dentener, F. J., Facchini, M. C., Van Dingenen, R., Ervens, B., Nenes, A., Nielsen, C. J., Swietlicki, E., Putaud, J. P., Balkanski, Y., Fuzzi, S., Horth, J., Moortgat, G. K.,
- 30 Winterhalter, R., Myhre, C. E. L., Tsigaridis, K., Vignati, E., Stephanou, E. G. and Wilson, J.: Organic aerosol and global climate modelling: a review, *Atmos. Chem. Phys.*, 5, 1053–1123, doi:10.5194/acp-5-1053-2005, 2005.
- Kidd, C., Perraud, V., Wingen, L. M. and Finlayson-Pitts, B. J.: Integrating phase and composition of secondary organic aerosol from the ozonolysis of alpha-pinene, *Proc. Natl. Acad. Sci. U. S. A.*, 111(21), 7552–7557, doi:10.1073/pnas.1322558111, 2014.
- 35 Koop, T., Bookhold, J., Shiraiwa, M. and Pöschl, U.: Glass transition and phase state of organic compounds: dependency on molecular properties and implications for secondary organic aerosols in the atmosphere, *Phys. Chem. Chem. Phys.*, 13(43), 19238–19255, doi:10.1039/c1cp22617g, 2011.

- Liu, P., Li, Y. J., Wang, Y., Gilles, M. K., Zaveri, R. A., Bertram, A. K. and Martin, S. T.: Lability of secondary organic particulate matter., *Proc. Natl. Acad. Sci. U. S. A.*, 113(45), 12643–12648, doi:10.1073/pnas.1603138113, 2016.
- Martin, S. T., Andreae, M. O., Althausen, D., Artaxo, P., Baars, H., Borrmann, S., Chen, Q., Farmer, D. K., Guenther, A., Gunthe, S. S., Jimenez, J. L., Karl, T., Longo, K., Manzi, A., Müller, T., Pauliquevis, T., Petters, M. D., Prenni, A. J., Pöschl, U., Rizzo, L. V., Schneider, J., Smith, J. N., Swietlicki, E., Tota, J., Wang, J., Wiedensohler, A. and Zorn, S. R.: An overview of the Amazonian Aerosol Characterization Experiment 2008 (AMAZE-08), *Atmos. Chem. Phys.*, 10(23), 11415–11438, doi:10.5194/acp-10-11415-2010, 2010.
- Pajunoja, A., Malila, J., Hao, L., Joutsensaari, J., Lehtinen, K. E. J. and Virtanen, A.: Estimating the Viscosity Range of SOA Particles Based on Their Coalescence Time, *Aerosol Sci. Technol.*, 48(August 2016), i–iv, doi:10.1080/02786826.2013.870325, 2014.
- Pathak, R. K., Stanier, C. O., Donahue, N. M. and Pandis, S. N.: Ozonolysis of alpha-pinene at atmospherically relevant concentrations: Temperature dependence of aerosol mass fractions (yields), *J. Geophys. Res. Atmos.*, 112(3), 1–8, doi:10.1029/2006JD007436, 2007.
- Perraud, V., Bruns, E. A., Ezell, M. J., Johnson, S. N., Yu, Y., Alexander, M. L., Zelenyuk, A., Imre, D., Chang, W. L., Dabdub, D., Pankow, J. F. and Finlayson-Pitts, B. J.: Nonequilibrium atmospheric secondary organic aerosol formation and growth, *Proc. Natl. Acad. Sci. U. S. A.*, 109(8), 2836–2841, doi:10.1073/pnas.1119909109, 2012.
- Pöschl, U., Martin, S. T., Sinha, B., Chen, Q., Gunthe, S. S., Huffman, J. A., Borrmann, S., Farmer, D. K., Garland, R. M., Helas, G., Jimenez, J. L., King, S. M., Manzi, A., Mikhailov, E., Pauliquevis, T., Petters, M. D., Prenni, A. J., Roldin, P., Rose, D., Schneider, J., Su, H., Zorn, S. R., Artaxo, P. and Andreae, M. O.: Rainforest aerosols as biogenic nuclei of clouds and precipitation in the Amazon., *Science*, 329(5998), 1513–6, doi:10.1126/science.1191056, 2010.
- Power, R. M. and Reid, J. P.: Probing the micro-rheological properties of aerosol particles using optical tweezers, *Reports Prog. Phys.*, 77(7), doi:10.1088/0034-4885/77/7/074601, 2014.
- Price, H. C., Mattsson, J. and Murray, B. J.: Sucrose diffusion in aqueous solution, *Phys. Chem. Chem. Phys.*, 18(28), 19207–19216, doi:10.1039/C6CP03238A, 2016.
- Pye, H. O. T. and Seinfeld, J. H.: A global perspective on aerosol from low-volatility organic compounds, *Atmos. Chem. Phys.*, 10(9), 4377–4401, doi:10.5194/acp-10-4377-2010, 2010.
- Pye, H. O. T., Chan, A. W. H., Barkley, M. P. and Seinfeld, J. H.: Global modeling of organic aerosol: The importance of reactive nitrogen (NO<sub>x</sub> and NO<sub>3</sub>), *Atmos. Chem. Phys.*, 10(22), 11261–11276, doi:10.5194/acp-10-11261-2010, 2010.
- Renbaum-Wolff, L., Grayson, J. W., Bateman, A. P., Kuwata, M., Sellier, M., Murray, B. J., Shilling, J. E., Martin, S. T. and Bertram, A. K.: Viscosity of alpha-pinene secondary organic material and implications for particle growth and reactivity, *Proc. Natl. Acad. Sci. U. S. A.*, 110(20), 8014–8019, doi:10.1073/pnas.1219548110, 2013.
- Riipinen, I., Pierce, J. R., Yli-Juuti, T., Nieminen, T., Hakkinen, S., Ehn, M., Junninen, H., Lehtipalo, K., Petaja, T., Slowik, J., Chang, R., Shantz, N. C., Abbatt, J., Leaitch, W. R., Kerminen, V. M., Worsnop, D. R., Pandis, S. N., Donahue, N. M. and Kulmala, M.: Organic condensation: a vital link connecting aerosol formation to cloud condensation nuclei (CCN) concentrations, *Atmos. Chem. Phys.*, 11(8), 3865–3878, doi:10.5194/acp-11-3865-2011,

- 2011.
- Saathoff, H., Naumann, K.-H., Moehler, O., Jonsson, A. M., Hallquist, M., Kiendler-Scharr, A., Mentel, T. F., Tillmann, R. and Schurath, U.: Temperature dependence of yields of secondary organic aerosols from the ozonolysis of alpha-pinene and limonene, *Atmos. Chem. Phys.*, 9(5), 1551–1577, doi:10.5194/acp-9-1551-2009, 2009.
- 5 Seinfeld, J. H. and Pandis, S. N.: *Atmospheric Chemistry and Physics*, 2nd Ed., John Wiley and Sons, Hoboken, NJ., 2006.
- Shiraiwa, M. and Seinfeld, J. H.: Equilibration timescale of atmospheric secondary organic aerosol partitioning, *Geophys. Res. Lett.*, 39, doi:10.1029/2012gl054008, 2012.
- Shiraiwa, M., Ammann, M., Koop, T. and Poschl, U.: Gas uptake and chemical aging of semisolid organic aerosol particles, *Proc. Natl. Acad. Sci. U. S. A.*, 108(27), 11003–11008, doi:10.1073/pnas.1103045108, 2011.
- Shiraiwa, M., Li, Y., Tsimpidi, A. P., Karydis, V. A., Berkemeier, T., Pandis, S. N., Lelieveld, J., Koop, T. and Pöschl, U.: Global distribution of particle phase state in atmospheric secondary organic aerosols, *Nat. Commun.*, doi:10.1038/ncomms15002, 2017.
- Song, M. J., Liu, P. F. F., Hanna, S. J., Zaveri, R. A., Potter, K., You, Y., Martin, S. T. and Bertram, A. K.: Relative humidity-dependent viscosity of secondary organic material from toluene photo-oxidation and possible implications for organic particulate matter over megacities, *Atmos. Chem. Phys.*, 16(14), 8817–8830, doi:10.5194/acp-16-8817-2016, 2016.
- Spracklen, D. V., Jimenez, J. L., Carslaw, K. S., Worsnop, D. R., Evans, M. J., Mann, G. W., Zhang, Q., Canagaratna, M. R., Allan, J., Coe, H., McFiggans, G., Rap, A. and Forster, P.: Aerosol mass spectrometer constraint on the global secondary organic aerosol budget, *Atmos. Chem. Phys.*, 11(23), 12109–12136, doi:10.5194/acp-11-12109-2011, 2011.
- Takegawa, N., Miyakawa, T., Kondo, Y., Jimenez, J. L., Zhang, Q., Worsnop, D. R. and Fukuda, M.: Seasonal and diurnal variations of submicron organic aerosol in Tokyo observed using the Aerodyne aerosol mass spectrometer, *J. Geophys. Res. Atmos.*, 111(11), 1–17, doi:10.1029/2005JD006515, 2006.
- 25 Wagner, N. L., Brock, C. A., Angevine, W. M., Beyersdorf, A., Campuzano-Jost, P., Day, D., De Gouw, J. A., Diskin, G. S., Gordon, T. D., Graus, M. G., Holloway, J. S., Huey, G., Jimenez, J. L., Lack, D. A., Liao, J., Liu, X., Markovic, M. Z., Middlebrook, A. M., Mikoviny, T., Peischl, J., Perring, A. E., Richardson, M. S., Ryerson, T. B., Schwarz, J. P., Warneke, C., Welti, A., Wisthaler, A., Ziemba, L. D. and Murphy, D. M.: In situ vertical profiles of aerosol extinction, mass, and composition over the southeast United States during SENEX and SEAC 4 RS: observations of a modest aerosol enhancement aloft, *Atmos. Chem. Phys.*, 15, 7085–7102, doi:10.5194/acp-15-7085-2015, 2015.
- 30 Wallace, J. M. and Hobbs, P. V.: *Atmospheric Science: An Introductory Survey*, Academic Press, Burlington, MA., 2006.
- Ye, Q., Robinson, E. S., Ding, X., Ye, P., Sullivan, R. C. and Donahue, N. M.: Mixing of secondary organic aerosols versus relative humidity, *Proc. Natl. Acad. Sci.*, 113(45), 12649–12654, doi:10.1073/pnas.1604536113, 2016.
- 35 Zaveri, R. A., Easter, R. C., Shilling, J. E. and Seinfeld, J. H.: Modeling kinetic partitioning of secondary organic aerosol and size distribution dynamics: representing effects of volatility, phase state, and particle-phase reaction, *Atmos. Chem. Phys.*, 14(10), 5153–5181, doi:10.5194/acp-14-5153-2014, 2014.

Zhang, Y., Sanchez, M. S., Douet, C., Wang, Y., Bateman, A. P., Gong, Z., Kuwata, M., Renbaum-Wolff, L., Sato, B. B., Liu, P. F., Bertram, A. K., Geiger, F. M. and Martin, S. T.: Changing shapes and implied viscosities of suspended submicron particles, *Atmos. Chem. Phys.*, 15(14), 7819–7829, doi:10.5194/acp-15-7819-2015, 2015.

Zobrist, B., Marcolli, C., Pedernera, D. A. and Koop, T.: Do atmospheric aerosols form glasses?, *Atmos. Chem. Phys.*, 8(17), 5221–5244, doi:10.5194/acp-8-5221-2008, 2008.

Formatted: Indent: Left: 0", Hanging: 0.5"

## Figures

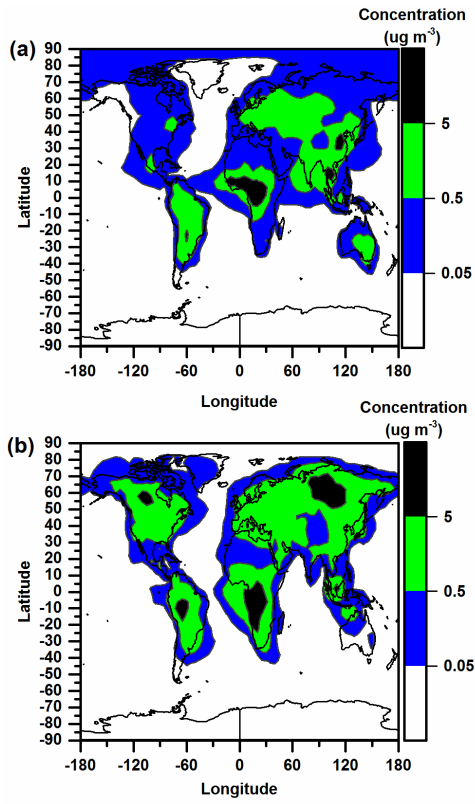


**Figure 1.** Monthly averaged  $\tau$ Total organic aerosol concentrations (color scale) at the Earth's surface in (a) January and (b) July, as calculated using GEOS-Chem.

5 [Average  \$\tau\$ Earth's](#)

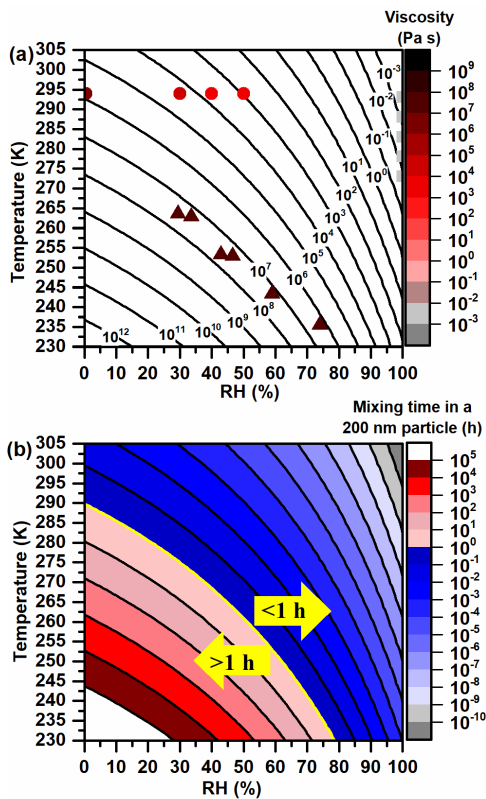


**Figure 22.** Plot of RH vs temperature with contour lines representing (a) our viscosity parameterization for  $\alpha$ -pinene SOA particles and (b) mixing times calculated for organic molecules with in 200 nm diameter  $\alpha$ -pinene SOA particles. The symbols in (a) represent the laboratory data used to develop the parameterization: squares represent the water viscosities from Crittenden et al. (2012); triangles represent the viscosity data of  $\alpha$ -pinene SOA from Järvinen et al. (2016) and the circles represent the viscosity data from Zhang et al. (2015), and the stars and pentagons represent the viscosity data from Grayson et al. (2016), measuring using SOA concentrations of 121 and 520  $\mu\text{g m}^{-3}$ , respectively. The 520  $\mu\text{g m}^{-3}$  data from Grayson et al. (2016) was offset by 5 K to improve visibility. The viscosity parameterization is based on  $\alpha$ -pinene SOA generated using mass concentrations of  $\sim 1000 \mu\text{g m}^{-3}$ .

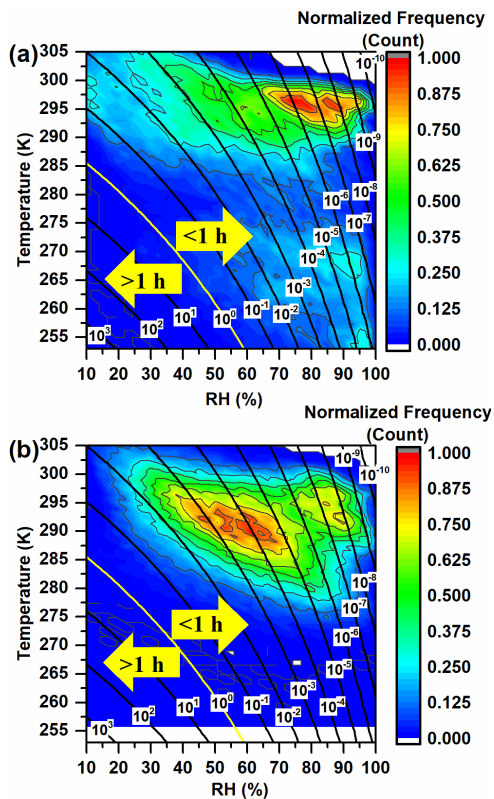


**Figure 33.** Six-hour normalized frequency counts of temperature and RH in the planetary boundary layer (PBL) (color scale) together with the mixing times for organic molecules within 200 nm  $\alpha$ -pinene SOA particles (contours). Panel A shows the conditions for January and panel B shows the conditions for July. Mixing times (contours) are reported

5 in hours. Frequency counts in the PBL were only included for the conditions where the mass concentration of total organic aerosol was  $> 0.5 \mu\text{g m}^{-3}$  at the surface. [The viscosity parameterization used to calculate mixing times was based on  \$\alpha\$ -pinene SOA generated using mass concentrations of  \$\sim 1000 \mu\text{g m}^{-3}\$ .](#)

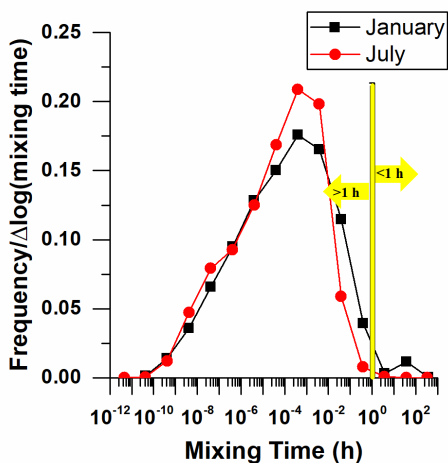


**Figure 44.** Normalized frequency distributions of mixing times within  $\alpha$ -pinene SOA in the planetary boundary layer (PBL). Black symbols correspond to January and red symbols corresponds to July. Frequency counts in the PBL were only included for the conditions where the mass concentration of total organic aerosol was  $> 0.5 \mu\text{g m}^{-3}$  at the surface.

- 5 [The viscosity parameterization used to calculate mixing times was based on  \$\alpha\$ -pinene SOA generated using mass concentrations of  \$\sim 1000 \mu\text{g m}^{-3}\$ .](#)

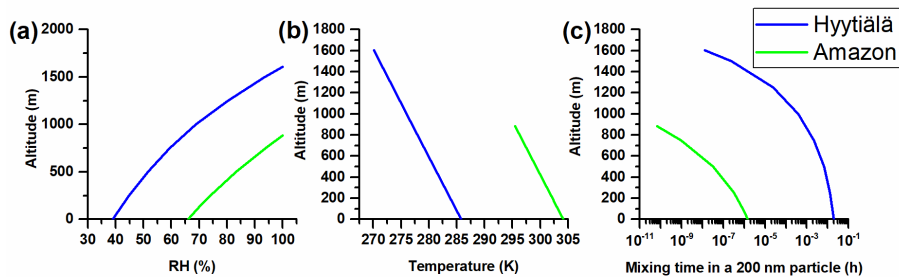
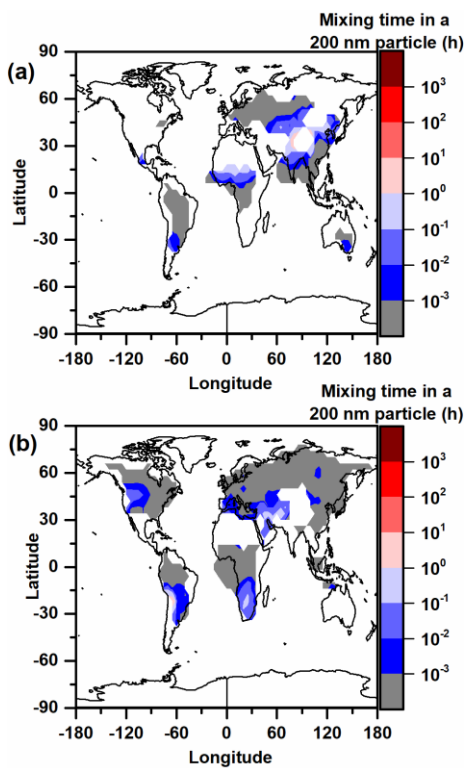
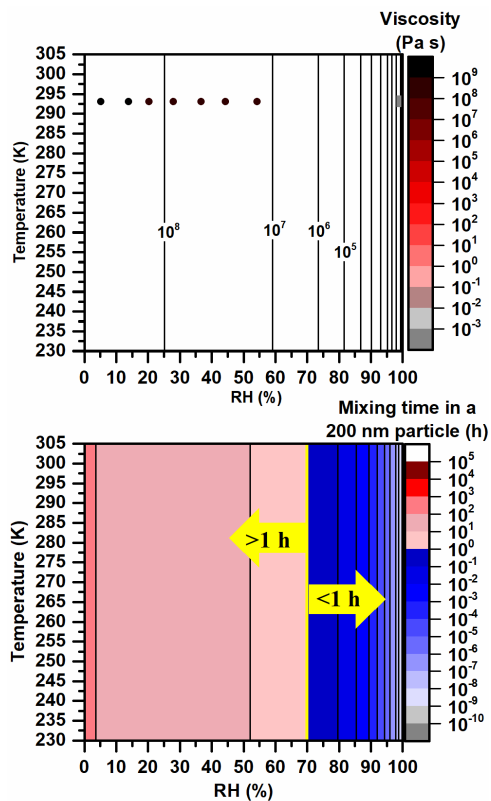


**Figure 55.** Temperature, RH and estimated mixing times for  $\alpha$ -pinene SOA as a function of altitude for Hyytiälä (boreal forest) and the Amazon (rainforest). The temperature and RH at ground level are the average afternoon values in the driest month of the year for the respective locations. The vertical profiles of temperature and RH are plotted until the RH is 100 % for these locations. The height at which RH reaches 100 % is only slightly lower than the average height of the planetary boundary layer predicted by GEOS-5 meteorology data. For details see the Supporting Information, Section [S2S1](#). [The viscosity parameterization used to calculate mixing times was based on  \$\alpha\$ -pinene SOA generated using mass concentrations of  \$\sim 1000 \mu\text{g m}^{-3}\$ .](#)



5 **Figure 66.** Mixing times of organic molecules within 200 nm  $\alpha$ -pinene SOA particles at the top of the planetary boundary layer as a function of latitudes and longitudes in (a) January and (b) July. The color scale represents mixing times, and the yellow contours illustrate when the concentration of total organic aerosols is  $\geq$  or  $<$  the mixing times are only shown for areas/locations with total organic aerosol concentrations  $\geq 0.5 \mu\text{g m}^{-3}$  at the surface. The viscosity parameterization used to calculate mixing times were based  $\alpha$ -pinene SOA generated using mass concentrations of

10  $\sim 1000 \mu\text{g m}^{-3}$ .



5 **Figure 7.** Plot of RH vs temperature with contour lines representing (a) the viscosity parameterization for  $\alpha$ -pinene SOA particles based on the data from Zhang et al. (2015) and (b) mixing times calculated for organic molecules within 200 nm diameter  $\alpha$ -pinene SOA particles. The symbols in (a) represent the laboratory data used to develop the parameterization: the square represents the water viscosity at room-temperature from Crittenden et al. (2012), and the circles represent the viscosity data from Zhang et al. (2015). The viscosity parameterization is based  $\alpha$ -pinene SOA generated using mass concentrations of  $\sim 70 \mu\text{g m}^{-3}$ .

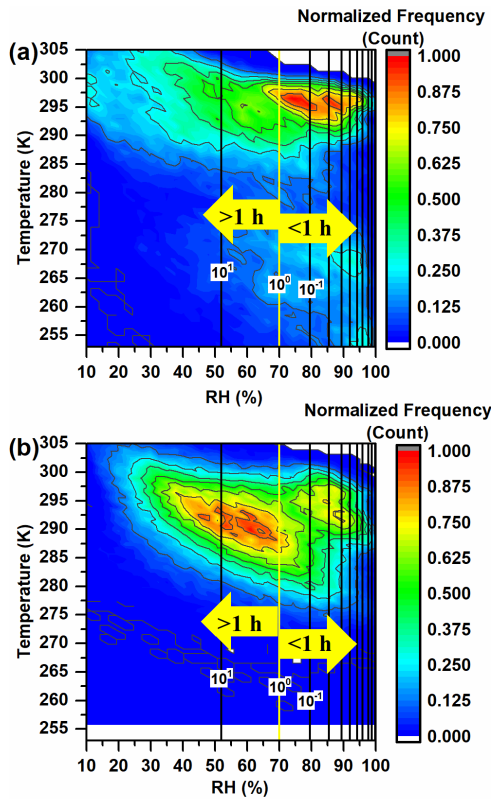


**Figure 8.** Six-hour normalized frequency counts of temperature and RH in the planetary boundary layer (PBL) (color scale) together with the mixing times for organic molecules within 200 nm  $\alpha$ -pinene SOA particles (contours) calculated based on the parameterization generated using the viscosities from Zhang et al. (2015). Panel A shows the conditions for January and panel B shows the conditions for July. Mixing times (contours) are reported in hours. Frequency counts in the PBL were only included for the conditions where the mass concentration of total organic aerosol was  $> 0.5 \mu\text{g m}^{-3}$  at the surface. The viscosity parameterization used to calculate mixing times was based on  $\alpha$ -pinene SOA generated using mass concentrations of  $\sim 70 \mu\text{g m}^{-3}$ .

10

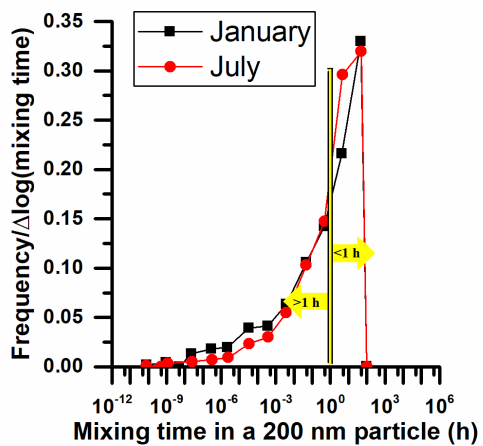


**Figure 9.** Normalized frequency distributions of mixing times within  $\alpha$ -pinene SOA in the planetary boundary layer (PBL) for the parameterization generated using the upper limit of the viscosity data from Zhang et al. (2015). Black symbols correspond to January and red symbols corresponds to July. Frequency counts in the PBL were only included for the conditions where the mass concentration of total organic aerosol was  $> 0.5 \mu\text{g m}^{-3}$  at the surface. The viscosity parameterization used to calculate mixing times was based on  $\alpha$ -pinene SOA generated using mass concentrations of  $\sim 70 \mu\text{g m}^{-3}$ .

10

15

20

Formatted: Not Superscript/ Subscript

# Mixing times of organic molecules within secondary organic aerosol particles: a global planetary boundary layer perspective

Adrian M. Maclean<sup>1</sup>, Christopher L. Butenhoff<sup>2</sup>, James W. Grayson<sup>1</sup>, Kelley Barsanti<sup>3</sup>, Jose L. Jimenez<sup>4\*</sup>, Allan K. Bertram<sup>1\*</sup>

<sup>1</sup>Department of Chemistry, University of British Columbia, Vancouver, BC, V6T 1Z1, Canada

<sup>2</sup>Dept. of Physics, Portland State University, Portland, Oregon

<sup>3</sup>Department of Chemical and Environmental Engineering and Center for Environmental Research and Technology, University of California, Riverside

<sup>4</sup>Cooperative Institute for Research in the Environmental Sciences and Department of Chemistry and Biochemistry, University of Colorado, Boulder, CO, USA

\*To whom correspondence should be addressed. Allan K. Bertram (email): [bertram@chem.ubc.ca](mailto:bertram@chem.ubc.ca) and Jose L. Jimenez (email): [jose.jimenez@colorado.edu](mailto:jose.jimenez@colorado.edu)

## Supporting Information

### S1. Derivation of Equation 1 from the main text.

The WLF equation provides a relationship between viscosity and temperature:

$$\log\left(\frac{\eta}{\eta_g}\right) = \frac{-C_1(T-T_g)}{C_2+(T-T_g)} \quad (S1)$$

where  $C_1$  and  $C_2$  are constants,  $T$  is the temperature,  $T_g$  is the glass transition temperature,  $\eta$  is the viscosity and  $\eta_g$  is the viscosity at the glass transition ( $10^{12}$  Pa s). The Gordon-Taylor equation provides a relationship between the glass transition temperature of a mixture and the weight fractions of its components:

$$T_{g,mix} = \frac{w_1 T_{g1} + w_2 T_{g2} k_{GT}}{w_1 + w_2 k_{GT}} \quad (S2)$$

where  $w_1$  and  $w_2$  are the weight fractions of the solute and water,  $T_{g1}$  and  $T_{g2}$  are the glass transition temperatures of the solute and water, and  $k_{GT}$  is a fitting parameter that describes the interaction between the two species. Equations (S1) and (S2) can be combined to give Eq. (1) in the main text. Equation (S1) (and hence Eq. (1)) is valid only at or above the glass transition temperature. As a result, we have not used Eq. (1) to predict viscosities  $> 10^{12}$  Pa s (which corresponds to mixing times  $> 5 \times 10^5$  h). This is not a concern for  $\alpha$ -pinene SOA since the viscosity of  $\alpha$ -pinene SOA is rarely  $> 10^{12}$  Pa s in the PBL.

**S2.1. Calculations of vertical profiles of temperature and RH in the boundary layer above Hyttiälä (boreal forest) and the Amazon (rainforest)**

The monthly average afternoon (13:00-15:00, local time) temperature and RH vertical profiles over Hyytiälä and the Amazon were calculated for the driest month of the year at these locations. For Hyytiälä, the average afternoon temperatures and RHs at the surface were obtained from the SMEAR II campaign data set for 2012, retrieved from Etsin Research data finder (https://etsin.avointiede.fi/dataset) (Aalto, 2012a, 2012b). For the Amazon, the temperature and RH at the surface ~~were~~ was obtained from NOAA's National Climate Data Center (http://www.ncdc.noaa.gov/) from 2004 to 2014, and an average from five different stations was used (Alfredo Vasquez Cobo, Itaituba, Tabatinga, Monte Dourado and Iauarete).

Formatted: Font: 12 pt

~~The vertical profiles of temperature were calculated using a dry adiabatic lapse rate of 9.8 K km<sup>-1</sup> and the average afternoon surface temperatures mentioned above. The temperature above the surface was calculated using a dry adiabatic lapse rate. The vertical profiles of RH were calculated using the average afternoon surface RHs mentioned above, the vertical profiles of temperature (calculated with the dry adiabatic lapse rate), and assuming the mixing ratio of water is independent of height in the PBL. rate of 9.8 K km<sup>-1</sup> and assuming that water vapour was well mixed within the PBL. It is expected that within the boundary layer, the mixing ratio will remain relatively constant with altitude and the temperature decrease will correspond to the adiabatic lapse rate (Fitzjarrald and Garstang, 1981; Stull, 2003; Turner et al., 2014). To determine the RH at different altitudes, For the calculations of RH as a function of altitude, the water vapor pressure and water saturated vapour pressure, were needed as a function of altitude. The water vapor pressure as a function of altitude was determined by multiplying the mixing ratio of water by the and atmospheric pressure were calculated. The atmospheric pressure, was calculated using the following equation (Seinfeld and Pandis, 2006):~~

Formatted: Font: 12 pt

$$P(z) = P_0 \exp\left(-\frac{Mgz}{kT}\right)$$

(S3S1)

where  $P_0$  is the standard pressure at sea level (101325 Pa),  $M$  is the molecular mass of the air (28.8 g/mol),  $g$  is the acceleration due to gravity (9.81 m s<sup>-2</sup>),  $z$  is the altitude in metres,  $k$  is the Boltzmann constant and  $T$  is the temperature in Kelvin. The water saturated vapour pressure was calculated as a function of attitude using the Antoine equation (National Institute of Standards and Technology, 2016):

Formatted: Font: 12 pt

$$\log_{10}(P) = A - \left(\frac{B}{T+C}\right) \quad (\text{S4S2})$$

where P is the pressure, A=4.6543, B=1435.264, C=-64.848 and T is the temperature in Kelvin. The values for A, B and C were based on the NIST values for water, which are valid for temperatures between 256 and 373 K (National Insitute of Standards and Technology, 2016).

Formatted: Font: 12 pt

In Fig. 5, the temperature and RH wereas plotted until the RH reached 100 %. The height at which RH reached 100 % was only slightly lower than the average height of the planetary boundary layer predicted by GEOS-5 meteorology data for the driest month of the year and for the afternoon (13:00-15:00, local time) above Hyytiälä and the Amazon. For Hyytiälä, 100 % RH was reached at 1605 m, while GEOS-5 predicted an average height of the PBL of 1667 m for this location and time. For the Amazon, 100 % RH was reached at 882 m, while GEOS-5 predicted an average height of the PBL of 1249 m for this location and time. When predicting the height of the PBL using GEOS-5 meteorology, we ran GEOS-Chem at a horizontal grid resolution of 2° latitude by 2.5° longitude rather 4° latitude by 4.5° longitude to provide a better approximation to these single locations. -ö

### S3S2. Parametrization for the viscosity of sucrose particles as a function of temperature and

#### 15 RH:

We developed a parameterization for viscosity of sucrose particles as function of temperature and RH by fitting the viscosity data listed in Table S5-S7 to the following equation:

$$\log(\eta) = 12 - \frac{C_1 * (T - \frac{w_{Suc} T_{gSuc} + w_{H2O} T_{gH2O} k_{GT}}{w_{Suc} + w_{H2O} k_{GT}})}{C_2 + (T - \frac{w_{Suc} T_{gSuc} + w_{H2O} T_{gH2O} k_{GT}}{w_{Suc} + w_{H2O} k_{GT}})} \quad (S5S3)$$

where C<sub>1</sub> and C<sub>2</sub> are constants, k<sub>GT</sub> is the Gordon-Taylor fitting parameter, T<sub>gSuc</sub> and T<sub>gH2O</sub> are the glass transition temperatures of dry sucrose and water and w<sub>Suc</sub> and w<sub>H2O</sub> are the weight fractions of the dry sucrose and water in the particles. The weight fractions of dry sucrose and water in the particles were determined from the RH using the following equation (Zobrist et al., 2011):

Field Code Changed

$$\frac{RH}{100} = \frac{1 + aw_{suc}}{1 + bw_{suc} + cw_{suc}^2} + (T - T^\theta)(dw_{suc} + ew_{suc}^2 + fw_{suc}^3 + gw_{suc}^4) \quad (S6S4)$$

where a-g are fitting parameters, T is the temperature in Kelvin and T<sup>θ</sup> is a reference temperature.

25 The values for T<sup>θ</sup> and a-g can be found in Table S6S8.

When fitting Eq. (S5S3) to the viscosity data for sucrose (Table S5S7), the parameters C<sub>1</sub>, C<sub>2</sub>, k<sub>GT</sub> and T<sub>gSuc</sub> were included as fitting parameters, while the glass transition temperature of water was fixed at 135 K (Longinotti and Corti, 2008). The values for these parameters retrieved by fitting

Field Code Changed

are reported in Table [S7S9](#). The  $T_{\text{g suc}}$  value obtained by fitting was within the range measured experimentally (319-335K) (Dette et al., 2014; Roos, 1993; Simperler et al., 2006).

Field Code Changed

Equation ([S5S3](#)) was based on the Williams, Landel and Ferry (WLF) equation and the Gordon-Taylor equation, similar to Eq. (1) in the main text. Since the WLF equation is only valid at or  
5 above the glass transition temperature, we have not used Eq. ([S5S3](#)) to predict viscosities above  $10^{12}$  Pa s (which corresponds to mixing times longer than  $5 \times 10^5$  h) (Fig. [S2S67](#)). If the temperature and RH in the PBL ~~were~~ such that the viscosity was greater than  $10^{12}$  Pa s, we assigned a viscosity of  $10^{12}$  Pa s and a mixing time of  $5 \times 10^5$  hours. This assignment does not affect the  
10 conclusions in this manuscript since a mixing time of  $5 \times 10^5$  hours is already well above the residence time of SOA particles in the atmosphere. However, this assignment did lead to a relatively large frequency count at  $5 \times 10^5$  hours in Fig. [S4S98](#).

## References

- Aalto, P.: Hyytiälä SMEAR II meteorology, gases and soil- Air temperature 8.4 m- 2012, atm-data@helsinki.fi, Etsin Res. data finder [online] Available from: <http://urn.fi/urn:nbn:fi:csc-kata20160308104539432017> (Accessed 28 June 2016a), 2012.
- Aalto, P.: Hyytiälä SMEAR II meteorology, gases and soil- Relative humidity 16 m-2012, atm-data@helsinki.fi, Etsin Res. data finder [online] Available from: <http://urn.fi/urn:nbn:fi:csc-kata20160308112058571248> (Accessed 28 June 2016b), 2012.
- 10 Crittenden, J. C., Trussel, R. R., Hand, D. W., Howe, K. J. and Tchobanoglous, G.: MWH's Water Treatment, John Wiley and Sons., 2012.
- Dette, H. P., Qi, M. A., Schroder, D. C., Godt, A. and Koop, T.: Glass-Forming Properties of 3-Methylbutane-1,2,3-tricarboxylic Acid and Its Mixtures with Water and Pinonic Acid, *J. Phys. Chem. A*, 118(34), 7024–7033, doi:10.1021/jp505910w, 2014.
- 15 Först, P., Werner, F. and Delgado, A.: On the pressure dependence of the viscosity of aqueous sugar solutions, *Rheol. Acta*, 41(4), 369–374, doi:10.1007/s00397-002-0238-y, 2002.
- Grayson, J. W., Zhang, Y., Mutzel, A., Renbaum-Wolff, L., Boege, O., Kamal, S., Herrmann, H., Martin, S. T. and Bertram, A. K.: Effect of varying experimental conditions on the viscosity of alpha-pinene derived secondary organic material, *Atmos. Chem. Phys.*, 16(10), 6027–6040, doi:10.5194/acp-16-6027-2016, 2016.
- 20 Järvinen, E., Ignatius, K., Nichman, L., Kristensen, T. B., Fuchs, C., Hoyle, C. R., Höppel, N., Corbin, J. C., Craven, J., Duplissy, J., Ehrhart, S., El Haddad, I., Frege, C., Gordon, H., Jokinen, T., Kallinger, P., Kirkby, J., Kiselev, A., Naumann, K. H., Petäjä, T., Pinterich, T., Prevot, A. S. H., Saathoff, H., Schiebel, T., Sengupta, K., Simon, M., Slowik, J. G., Tröstl, J., Virtanen, A.,
- 25 Vochezer, P., Vogt, S., Wagner, A. C., Wagner, R., Williamson, C., Winkler, P. M., Yan, C., Baltensperger, U., Donahue, N. M., Flagan, R. C., Gallagher, M., Hansel, A., Kulmala, M., Stratmann, F., Worsnop, D. R., Möhler, O., Leisner, T. and Schnaiter, M.: Observation of viscosity transition in  $\alpha$ -pinene secondary organic aerosol, *Atmos. Chem. Phys.*, 16(7), 4423–4438, doi:10.5194/acp-16-4423-2016, 2016.
- 30 Longinotti, M. P. and Corti, H. R.: Viscosity of concentrated sucrose and trehalose aqueous solutions including the supercooled regime, *J. Phys. Chem. Ref. Data*, 37(3), 1503–1515, doi:10.1063/1.2932114, 2008.
- Migliori, M., Gabriele, D., Di Sanzo, R., De Cindio, B. and Corraera, S.: Viscosity of multicomponent solutions of simple and complex sugars in water, *J. Chem. Eng. Data*, 52(4), 1347–1353, doi:10.1021/je700062x, 2007.
- 35 National Institute of Standards and Technology: Water, [online] Available from: <http://webbook.nist.gov/cgi/cbook.cgi?ID=C7732185&Mask=4&Type=ANTOINE&Plot=on#ANTOINE> (Accessed 1 August 2016), 2016.
- Perry, R. and Green, D.: Perry's Chemical Engineers' Handbook, McGraw-Hill, Toronto., 2008.
- 40 Power, R. M. and Reid, J. P.: Probing the micro-rheological properties of aerosol particles using optical tweezers, *Reports Prog. Phys.*, 77(7), doi:10.1088/0034-4885/77/7/074601, 2014.
- Quintas, M., Brandão, T. R. S., Silva, C. L. M. and Cunha, R. L.: Rheology of supersaturated sucrose solutions, *J. Food Eng.*, 77(4), 844–852, doi:10.1016/j.jfoodeng.2005.08.011, 2006.
- Roos, Y.: Melting and glass transitions weight carbohydrates of low molecular, *Carbohydr. Res.*, 45 238, 39–48, doi:10.1016/0008-6215(93)87004-C, 1993.

Field Code Changed

Seinfeld, J. H. and Pandis, S. N.: Atmospheric Chemistry and Physics, 2nd Ed., John Wiley and Sons, Hoboken, NJ., 2006.

Simperler, A., Kornherr, A., Chopra, R., Bonnet, P. A., Jones, W., Motherwell, W. D. S. and Zifferer, G.: Glass transition temperature of glucose, sucrose, and trehalose: An experimental and in silico study, J. Phys. Chem. B, 110(39), 19678–19684, doi:10.1021/jp063134t, 2006.

Song, M. J., Liu, P. F. F., Hanna, S. J., Zaveri, R. A., Potter, K., You, Y., Martin, S. T. and Bertram, A. K.: Relative humidity-dependent viscosity of secondary organic material from toluene photo-oxidation and possible implications for organic particulate matter over megacities, Atmos. Chem. Phys., 16(14), 8817–8830, doi:10.5194/acp-16-8817-2016, 2016.

10 Swindells, J. F. and States., U.: Viscosities of sucrose solutions at various temperatures: tables of recalculated values, , 7 [online] Available from: file://catalog.hathitrust.org/Record/007290919, 1958.

Telis, V. R. N., Telis-Romero, J., Mazzotti, H. B. and Gabas, a. L.: Viscosity of Aqueous Carbohydrate Solutions at Different Temperatures and Concentrations, Int. J. Food Prop., 10(1), 15 185–195, doi:10.1080/10942910600673636, 2007.

Zhang, Y., Sanchez, M. S., Douet, C., Wang, Y., Bateman, A. P., Gong, Z., Kuwata, M., Renbaum-Wolff, L., Sato, B. B., Liu, P. F., Bertram, A. K., Geiger, F. M. and Martin, S. T.: Changing shapes and implied viscosities of suspended submicron particles, Atmos. Chem. Phys., 15(14), 7819–7829, doi:10.5194/acp-15-7819-2015, 2015.

20 Zobrist, B., Marcolli, C., Pedernera, D. A. and Koop, T.: Do atmospheric aerosols form glasses?, Atmos. Chem. Phys., 8(17), 5221–5244, doi:10.5194/acp-8-5221-2008, 2008.

Zobrist, B., Soonsin, V., Luo, B. P., Krieger, U. K., Marcolli, C., Peter, T. and Koop, T.: Ultra-slow water diffusion in aqueous sucrose glasses, Phys. Chem. Chem. Phys., 13(8), 3514–3526, doi:10.1039/c0cp01273d, 2011.

25 **Tables**

30 **Table S1.** Room-temperature  $\alpha$ -pinene SOA viscosity data ~~used from Grayson et al. (2016).~~ ~~Viscosity data corresponds to SOA generated with a mass concentration of 520  $\mu\text{g m}^{-3}$ .~~ ~~to create a parameterization for the viscosity of  $\alpha$ -pinene SOA as a function of temperature and RH.~~

Reference	Viscosity (Pa s)	RH (%)	Temperature (K)
Grayson et al. (2016) (SOA generated with a mass concentration = 520 $\mu\text{g m}^{-3}$ )	<sup>a</sup> Range=4.2x10 <sup>2</sup> -3.1x10 <sup>4</sup> , midpoint=3.6x10 <sup>3</sup> <sup>a</sup> Range=1.8x10 <sup>2</sup> -1.5x10 <sup>4</sup> , midpoint=1.6 x10 <sup>3</sup>	5050	<sup>c</sup> Range=293-295 Midpoint=294 <sup>e</sup> Range=293-295 Midpoint=294
<sup>3</sup> Grayson et al. (2016) (SOA generated with mass concentration =121 $\mu\text{g m}^{-3}$ )	<sup>a</sup> Range=9.7x10 <sup>2</sup> -7.9x10 <sup>4</sup> , midpoint=8.7x10 <sup>3</sup> <sup>a</sup> Range=9.8x10 <sup>2</sup> -3.0x10 <sup>4</sup> , midpoint=5.4 x10 <sup>3</sup>	4040	
	<sup>a</sup> Range=3.4x10 <sup>3</sup> -2.1x10 <sup>5</sup> , midpoint=2.6x10 <sup>4</sup> <sup>a</sup> Range=4.6x10 <sup>3</sup> -1.4x10 <sup>5</sup> , midpoint=2.5x10 <sup>4</sup>	3030	
	<sup>a</sup> Range=3.5x10 <sup>5</sup> -1.8x10 <sup>7</sup> , midpoint=2.5x10 <sup>6</sup> <sup>a</sup> Range=1.6x10 <sup>6</sup>	<sup>b</sup> 0 <sup>b</sup> 0	

Formatted: Left, Line spacing: single

Field Code Changed

Field Code Changed

Formatted: Font: (Default) Times New Roman

Formatted: Font: (Default) Times New Roman

	$-5.9 \times 10^7$ ; midpoint= $9.6 \times 10^6$		
Bateman et al. (2015)	$1 \times 10^4$	70	293

<sup>a</sup> Grayson et al. (2016) reported upper and lower limits to the viscosity (i.e. range) at each specified RH. To simplify the fitting procedure, we used the midpoints of the viscosities from Grayson et al (2016).

Field Code Changed

<sup>b</sup> Grayson et al. (2016) measured the viscosity under dry conditions (RH of < 0.5 % based on measurements). When developing the ~~parameterization~~parameterization, we used a value of 0 % RH.

Field Code Changed

Field Code Changed

<sup>c</sup> Grayson et al. (2016) carried out experiments at room temperature (293 K-295 K). We used the midpoint of the temperature (294 K) when developing the viscosity parameterization for  $\alpha$ -pinene SOA.

Field Code Changed

~~<sup>d</sup>Zhang et al. (2015) reported 36 measurements of viscosity over the range of 0 to 60%. For the fitting procedure, we binned their data by relative humidity and used the average viscosity and relative humidity in each bin. The width of each bin was approximately 10% RH. This binning procedure was carried out to give the data from Grayson et al. (2016) and Zhang et al. (2015) similar weights, since both were carried out at room temperature and over a similar RH range.~~

**Table S2S2.** Low-temperature  $\alpha$ -pinene SOA viscosity data from Järvinen et al. (2016). Viscosity data corresponds to SOA generated with a mass concentration of 707-1414  $\mu\text{g m}^{-3}$ . used to create a parameterization for the viscosity of  $\alpha$ -pinene SOA as a function of temperature and RH.

Formatted: Font: 12 pt

Field Code Changed

Formatted: Font: 12 pt

Formatted: Font: 12 pt

Reference	Viscosity (Pa s)	RH (%)	Temperature (K)
Järvinen et al. (2016)	$1 \times 10^7$	<sup>a</sup> Range=22.9-36.3, midpoint=29.6	263.3
		<sup>a</sup> Range=30.5-37.3, midpoint=33.9	262.9
		<sup>a</sup> Range=40.5-46.0, midpoint=43.3	253.3
		<sup>a</sup> Range=44.0-49.8, midpoint=46.9	252.9
		<sup>a</sup> Range=55.0-63.4, midpoint=59.2	243.3
		<sup>a</sup> Range=68.6-80.1, midpoint=74.4	235.5

Field Code Changed

<sup>a</sup> Järvinen et al (2016) reported upper and lower limits to the RH for a specific temperature and viscosity. To simplify fitting, we used the midpoint of the RH range.

Field Code Changed

**Table S3S3.** Liquid water viscosity data from Crittenden et al. (2012) used to create a parameterization for the viscosity of  $\alpha$ -pinene SOA as a function of temperature and RH.

Reference	Viscosity (Pa s)	RH (%)	Temperature (K)
Crittenden et al. (2012)	<sup>a</sup> 1.002x10 <sup>-3</sup>	100	293
	<sup>a</sup> 1.139 x10 <sup>-3</sup>		288
	<sup>a</sup> 1.307 x10 <sup>-3</sup>		283
	<sup>a</sup> 1.518 x10 <sup>-3</sup>		278
	<sup>a</sup> 1.781 x10 <sup>-3</sup>		273

<sup>a</sup> The viscosity values in Crittenden et al. (2012) were reported to 4 significant digits.

**Table S4S4.** Initial guess parameters and fitting parameters used in Eq. (1) to predict the viscosity of  $\alpha$ -pinene SOA as a function of temperature and RH. The fitting parameters were obtained by fitting Eq. (1) to the viscosity data listed in Tables S1-S3.

Parameter	Guess Value	Fitting Value
C <sub>1</sub>	19	31297131
C <sub>2</sub>	50 K	3314461165 K
K <sub>GT</sub>	2.5	5.1553.934
T <sub>gSOA</sub>	250 K	245.17236.8 K

10 **Table S5.** Room temperature  $\alpha$ -pinene SOA viscosity data from Zhang et al. (2015). Viscosity data corresponds to SOA generated with a mass concentration of  $\sim 70 \mu\text{g m}^{-3}$ . used to create a parameterization for the viscosity of  $\alpha$ -pinene SOA as a function of temperature and RH to investigate the impact of mass loading.

Reference	Viscosity (Pa s)	RH (%)	Temperature (K)
Zhang et al. (2015) <sup>a</sup>	$2.3 \times 10^8$	5.2	293
	$1.3 \times 10^8$	13.8	293
	$3.2 \times 10^7$	22.9	293
	$1.4 \times 10^7$	36.7	293
	$6.0 \times 10^6$	44.3	293
	$5.1 \times 10^6$	54.3	293

15 <sup>a</sup>Zhang et al. (2015) reported 36 measurements of viscosity over the range of 0 to 60 %. For the fitting procedure, we binned their data by relative humidity and used the average viscosity and relative humidity in each bin. The width of each bin was approximately 10 % RH.

~~This binning procedure was carried out to give the data from Grayson et al. (2016) and Zhang et al. (2015) similar weights, since both were carried out at room temperature and over a similar RH range.~~

~~Table S6. Initial guess parameters and fitting parameters used in Eq. (1) to predict develop a temperature-independent parameterization for viscosity of the viscosity of  $\alpha$ -pinene SOA. The fitting parameters were obtained by fitting Eq. (1) to the room-temperature viscosity data from Zhang et al. (Zhang et al., 2015) and Crittenden et al. (2012), but with the temperature (T) in Eq. (1) replaced by 293 K. A as a function of temperature and RH for the upper limit of the Zhang et al. ((Zhang et al., 2015) viscosity data.~~

Parameter	Guess Value	Fitting Value
$C_1$	19	18.73
$C_2$	50 K	29.25
$K_{GT}$	2.5	0.1628
$T_{gSOA}$	250 K	285.9 K

Table S5S7. Literature viscosity data used to create a parameterization for the viscosity of sucrose particles as a function of temperature and RH.

System	Viscosity Range (Pa s)	RH (%)	Temperature (K)	Reference
Water	$1.002 \times 10^{-3}$ to $1.781 \times 10^{-3}$	100	275-293	Crittenden et al. (2012)
Sucrose-water	$3.19 \times 10^{-3}$ to $4.82 \times 10^{-1}$	96.2-80	293	Swindells et al. (1958)
	$6.73 \times 10^{-1}$ to $1.10 \times 10^3$	80-56.6		Quintas et al. (2006)
	$1.97 \times 10^{-3}$ to $5.67 \times 10^{-2}$	99.4-88		Perry and Green (2008)
	$1.25 \times 10^{-3}$ to $8.30 \times 10^{-2}$	99.99-87.96		Migliori et al. (2007)
	$1.26 \times 10^{-3}$ to $7.65 \times 10^{-2}$	99.89-87.98		Telis et al. (2007)
	$1.03 \times 10^{-3}$ to $5.81 \times 10^{-2}$	100-87.98		Forst et al. (2002)

Commented [AM2]: Is this still a valid statement since we are no longer using them both in the same parameterization?

Formatted: Font: 12 pt

Formatted: Font: Not Bold

Formatted: Font: 12 pt

Formatted: Font: 12 pt

Field Code Changed

Formatted: Font: 12 pt

Formatted: Font: 12 pt

Formatted: Font: 12 pt

Formatted: Font: Bold

Formatted: Font: Bold

Formatted: Font: Bold

Formatted Table

Formatted: Font: 12 pt

Formatted: Left

Field Code Changed

	$3 \times 10^{-2}$ to $6.71 \times 10^8$	92-28		Power and Reid (2014)
	$1 \times 10^{12}$	48.53-25.88	255-295 (5 degree increments) <sup>a</sup>	Zobrist et al. (2008)

Field Code Changed

Field Code Changed

Field Code Changed

<sup>a</sup> Zobrist et al. (2008) reported glass transition temperatures as a function of water activity for the range of 160 K to 300 K. These glass transition temperatures were based on glass transition temperature measurements in the range of 180-240 K to 240-180 K, water activity measurements, and the Gordon-Taylor equation. To develop our parameterization, we used their glass transition temperatures over the range of 255 K to 295 K from their Fig. 5b, recorded in 5 K increments.

**Table S6S8.** Parameters from Zobrist et al. (2011) used in Eq. (S46) to predict the weight fractions of sucrose and water in particles as a function of relative humidity.

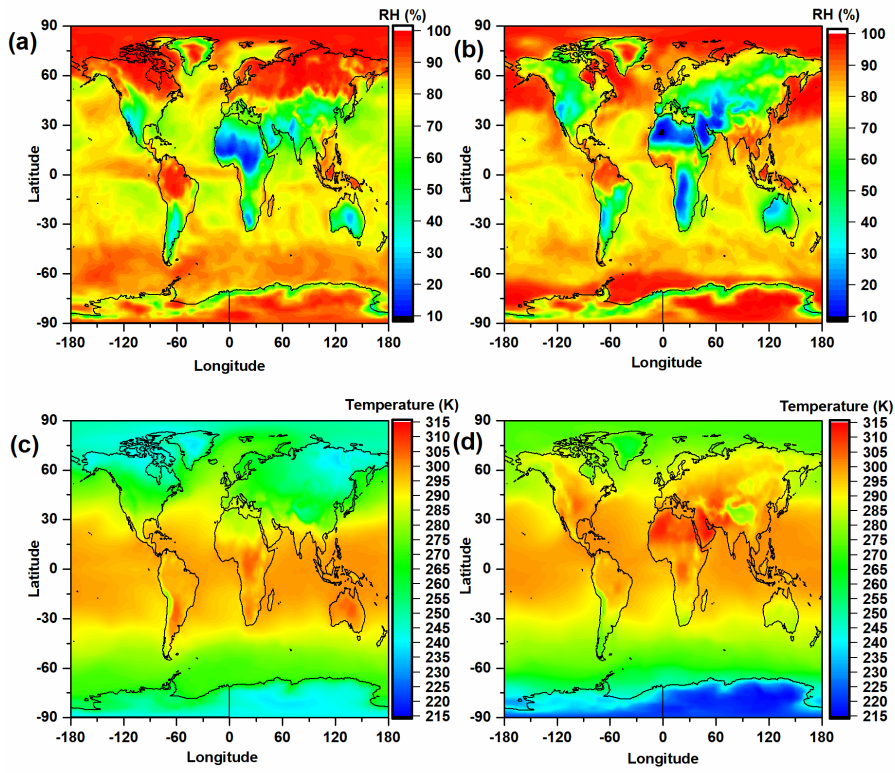
Field Code Changed

Parameter	Value	Parameter	Value
a	-1	e	-0.005151
b	-0.99721	f	0.009607
c	0.13599	g	-0.006142
d	0.001688	T <sup>o</sup>	298 K

10 **Table S7S9.** Fitting parameters used in Eq. (S35) to predict the viscosity of sucrose particles as a function of temperature and RH. These parameters were obtained by fitting Eq. (S35) to the viscosity data listed in Table S5-S76 as well as the guess values in the table.

Parameter	Guess Value	Fitting Value
C <sub>1</sub>	19	20.06
C <sub>2</sub>	50 K	55.58 K
K <sub>GT</sub>	4.74	4.531
T <sub>gSOA</sub>	336 K	324.5 K

Figures



Formatted: Font: 12 pt

**Figure S1. Monthly averaged relative humidity and temperature at the surface. Panels (a) and**

Formatted: Font: 12 pt, Bold

5 (c) correspond to January and panels (b) and (d) correspond to July.

Formatted: Font: 12 pt

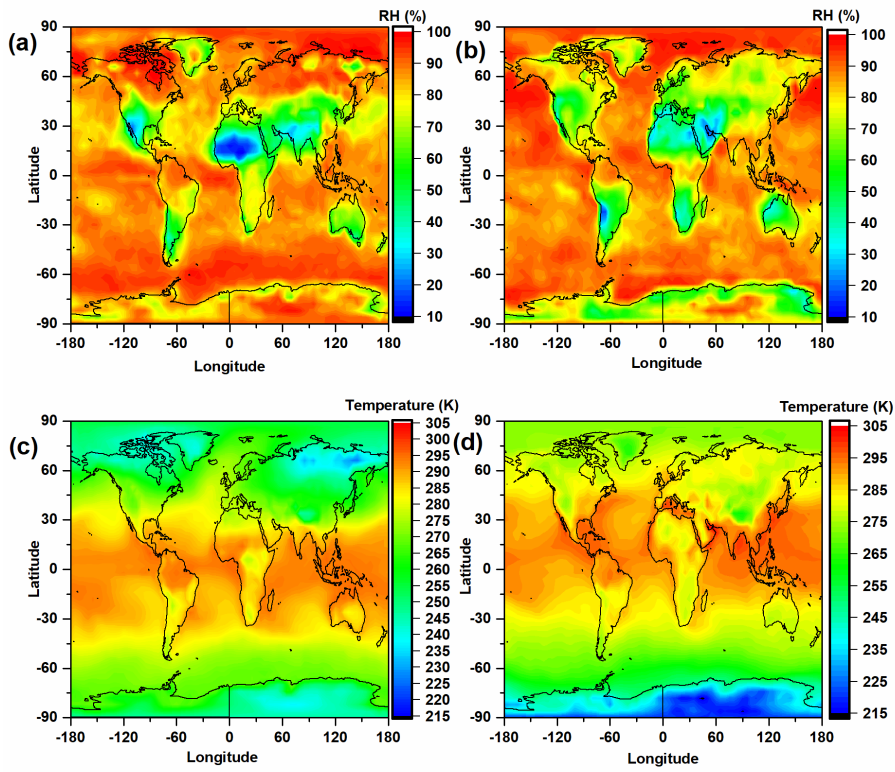


**Figure S2.** Monthly average relative humidity and temperature at the top of the planetary boundary layer. Panels (a) and (c) correspond to January, and panels (b) and (d) correspond to July.

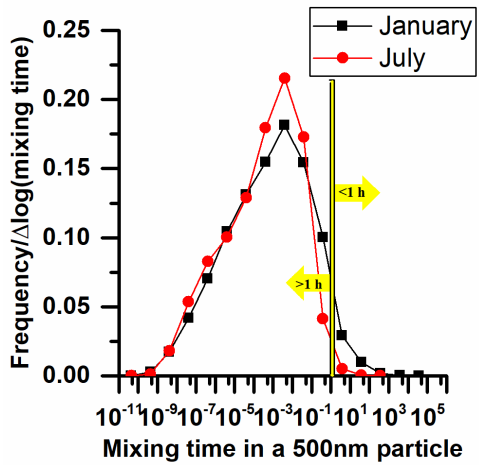
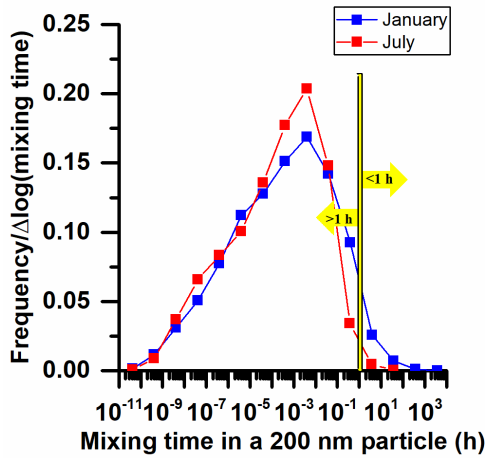


**Figure S3.** Normalized frequency distributions of mixing times within 500 nm  $\alpha$ -pinene SOA -with a diameter of 500 nm- in the planetary boundary layer (PBL). Black symbols correspond to January and red symbols corresponds to July. Frequency counts in the PBL were only included for the conditions where the mass concentration of total organic aerosol was  $> 0.5 \mu\text{g m}^{-3}$  at the surface. The viscosity parameterization used to calculate mixing times was based on  $\alpha$ -pinene SOA generated using mass concentrations of  $\sim 1000 \mu\text{g m}^{-3}$ .



Formatted: Font: 12 pt

**Figure S4.** Normalized frequency distributions of mixing times within  $\alpha$ -pinene SOA in the planetary boundary layer (PBL) in January for the parameterizations generated using the upper limit of the viscosity data from Grayson et al. (Grayson et al., 2016) and the upper RH limit from Järvinen et al. (2016). Blue symbols correspond to January and red symbols correspond to July.

5 Frequency counts in the PBL were only included for the conditions where the mass concentration of total organic aerosol was  $> 0.5 \mu\text{g m}^{-3}$  at the surface.

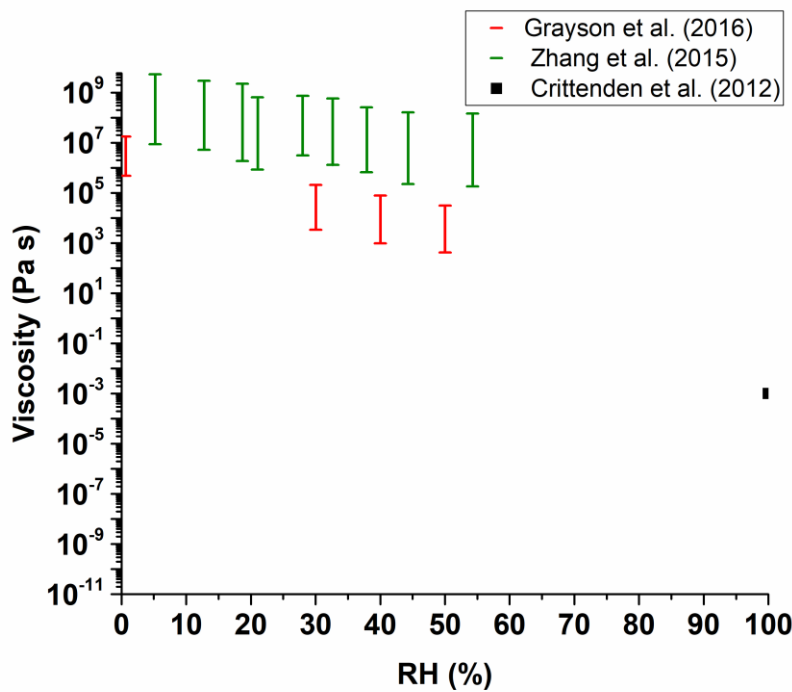


**Figure S5.** Viscosities of  $\alpha$ -pinene particles as a function of different RHs from Zhang et al. (Zhang et al., 2015) and Grayson et al. (Grayson et al., 2016), as well as the viscosity of water at room temperature from Crittenden et al. (Crittenden et al., 2012). The viscosity data from Grayson et al. (2016) correspond to a SOA mass concentration of  $520 \mu\text{g m}^{-3}$ , and the viscosity data from Zhang et al. (2015) correspond to a SOA mass concentration of  $70 \mu\text{g m}^{-3}$ . performed viscosity measurements on SOA particles generated at a mass concentration of  $520 \mu\text{g m}^{-3}$  and Zhang et al. (2015) used a mass concentration of  $70 \mu\text{g m}^{-3}$ .

10

Formatted: Font: 12 pt  
 Formatted: Font: 12 pt  
 Formatted: Font: 12 pt  
 Field Code Changed

Formatted: Font: 12 pt  
 Formatted: Font: 12 pt

Formatted: Font: 12 pt  
 Formatted: Font: 12 pt  
 Formatted: Font: 12 pt  
 Formatted: Font: 12 pt  
 Formatted: Font: 12 pt  
 Formatted: Font: 12 pt

Commented [AB3]: Make sure the second panel does not suggest a temperature dependence.

Formatted: Font: 12 pt  
 Formatted: Font: 12 pt

Commented [AB4]: Add these figures to the main text.

Formatted: Font: 12 pt  
 Formatted: Font: 12 pt  
 Formatted: Font: 12 pt

Commented [AB5]: Add this figure to the main text.  
 Formatted: Font: 12 pt  
 Formatted: Font: 12 pt

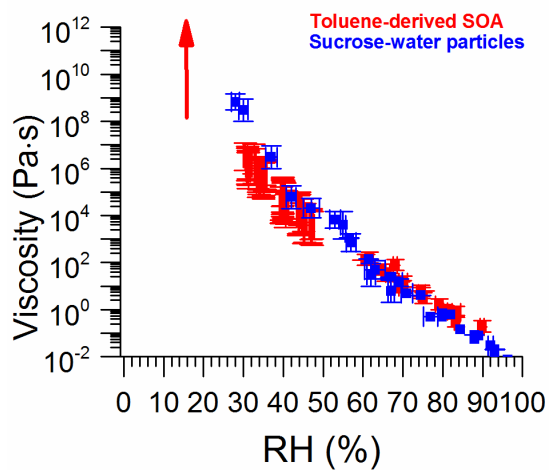


**Figure S1S6.** Viscosities of different proxies of anthropogenic SOA as a function of RH. Data for toluene SOA taken from Song et al. (2016). The data for sucrose-water mixtures was taken from Swindells (1958), Quintas et al. (2006), Telis et al. (2007), Forst et al. (2002), Migliori et al. (2007), Perry and Green (2008), and Power and Reid (2014).

- Formatted: Font: 12 pt

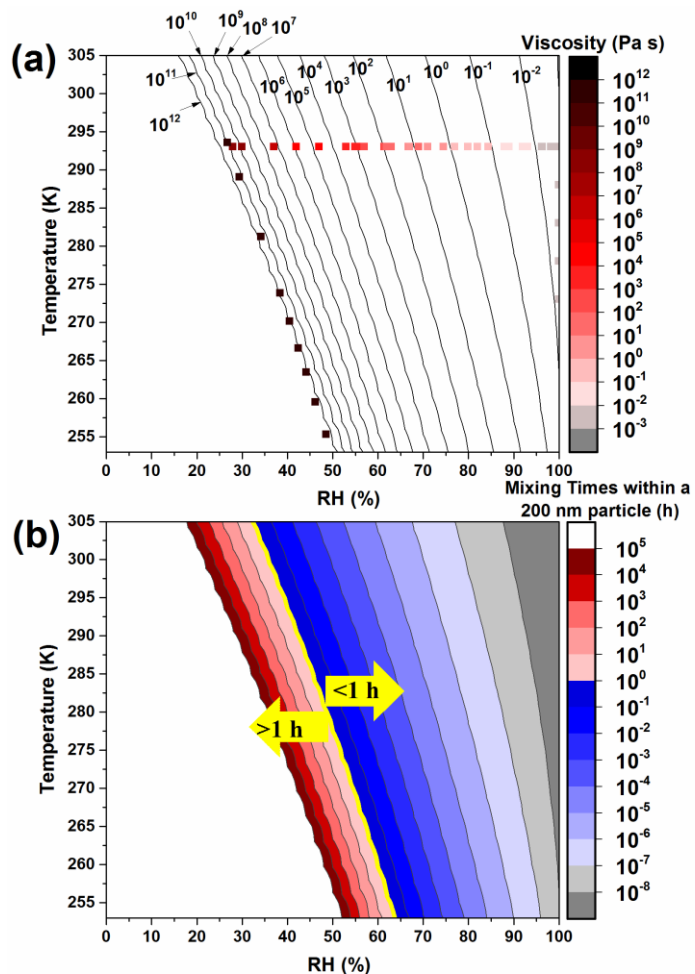


**Figure S2S7.** Panel A: Parameterization (contours) for the viscosity of sucrose particles (as surrogates of ~~toluene-anthropogenic~~ SOA) as a function of temperature and RH and measured viscosities used to construct the parameterization (symbols). The measured viscosities are listed in Table S5S76. Panel B: Mixing times (color scale) for organic molecules within 200 nm sucrose particles as a function of temperature and RH. Mixing times were calculated from the viscosity parameterization (Panel A) and Eq. (53) and (64) in the main text.

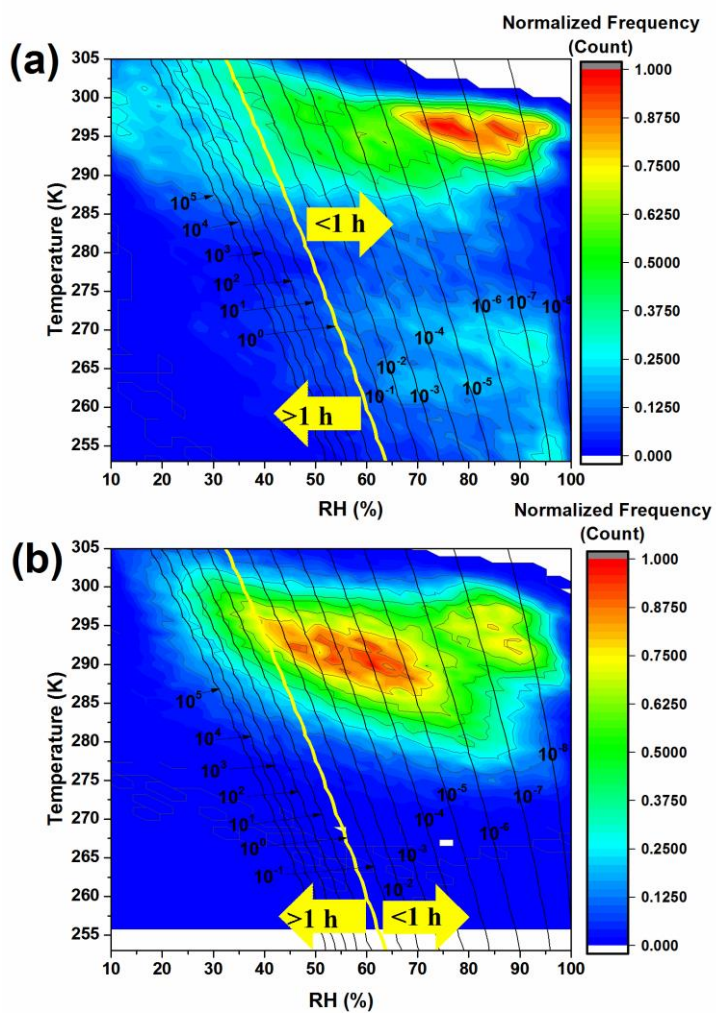
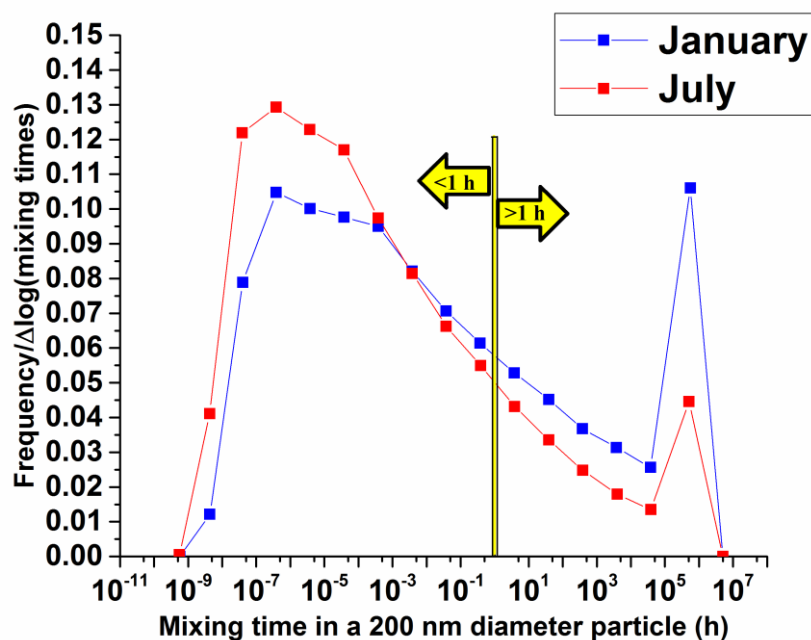
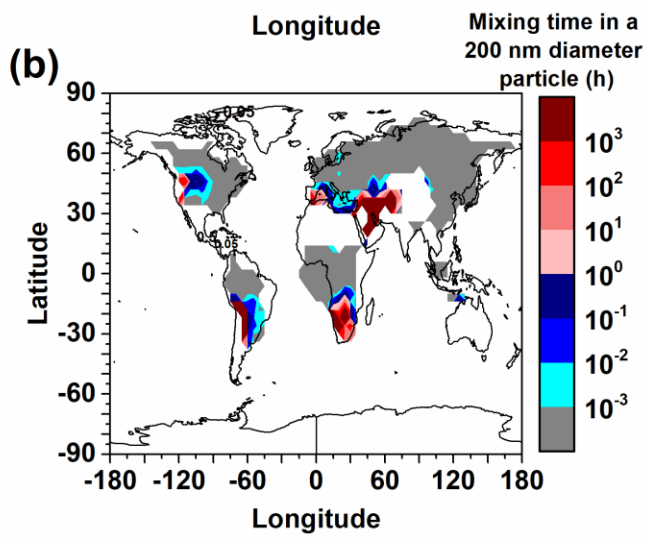
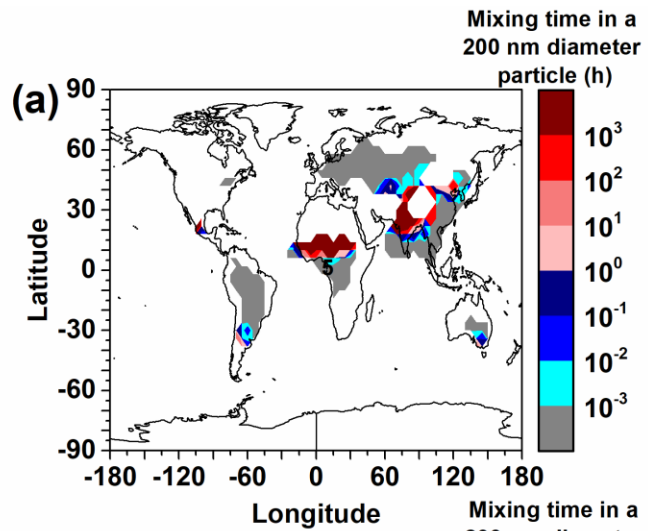


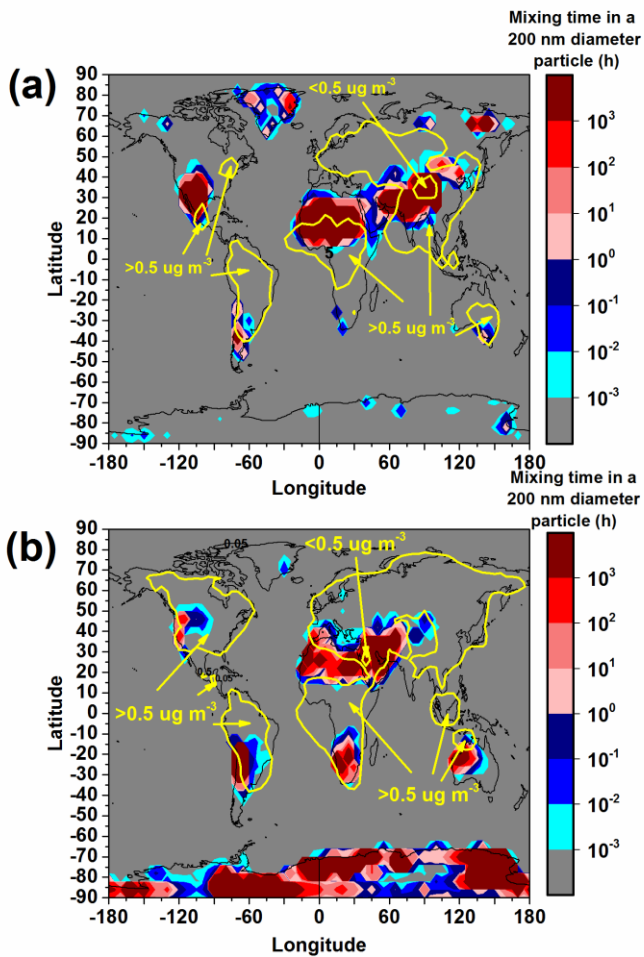
Figure S3S8. Six-hour normalized frequency counts of temperature and RH in the planetary boundary layer (color scale) together with the mixing times for organic molecules within 200 nm sucrose particles (as surrogates of ~~toluene~~-anthropogenic SOA) (contours). Panels A and B show the conditions for January and July, respectively. Mixing times (contours) are reported in hours.

Frequency counts in the PBL were only included for the conditions when the mass concentration of total organic aerosol was  $> 0.5 \mu\text{g}/\text{m}^3$  at the surface.



5 **Figure S4S9.** Normalized frequency distributions of mixing times within sucrose particles (as  
surrogates for ~~toluene~~-anthropogenic SOA) in the planetary boundary layer. Red symbols  
corresponds correspond to January and blue symbols corresponds to July. Frequency counts in the  
PBL were only included for the conditions where the mass concentration of total organic aerosol  
was  $> 0.5 \mu\text{g m}^{-3}$  at the surface. The relatively large frequency count at  $5 \times 10^5 \text{ h}$  is because all cases  
10 that had a viscosity greater than  $10^{12} \text{ Pa s}$  ~~were assigned, it was assigned~~ a value of  $10^{12} \text{ Pa s}$ . For  
additional details see Section S23.





**Commented [AB6]:** This figure should be modified like the figure in the main text. I.e. only show colors for conditions where OA <math>< 0.5 \text{ micrograms/m}^3</math>

**Formatted:** Font: 12 pt

**Figure S5S10.** Mixing times of organic molecules within 200 nm sucrose particles (as surrogates of ~~to~~ luene-anthropogenic SOA) at the top of the planetary boundary layer as a function of latitude and longitude. The color scale represents mixing times. Mixing times are only shown for locations  
 5 with total organic aerosol concentrations >math>0.5 \mu\text{g m}^{-3}</math> at the surface. The color scale represents

**Formatted:** Font: 12 pt

**Formatted:** Font: 12 pt

**Formatted:** Font: 12 pt

mixing times and the yellow contours illustrate when the concentration of total organic aerosol is  $> 0.5 \mu\text{g m}^{-3}$  at the surface. Panels A and B correspond to January and July, respectively.